2f, which is that the PCNA molecules, just encircled on DNA, are not efficient targets for ubiquitination, but rather PCNA molecules, proximately located at the 3′-end and making complex with pol δ as illustrated in Fig. 4f. We suggest that stimulation of ubiquitination by DNA synthesis was mainly a consequence of continuous loading of PCNA onto the DNA and subsequent ubiquitination of the newly loaded PCNA molecules.

Reconstitution of DNA replication on a damaged template with polymerase switching between pol δ and pol η

It is critical to ask whether polymerase switching reactions between pol δ and translesion pols are observed in this *in vitro* system. To reconstitute polymerase switching, we used UV-irradiated mp18 ssDNA as a template. First, mp18 ssDNA was irradiated with different doses of UV (50–1600 J/m^2) after which its capacity as a template for replication with pol δ was examined (Supplementary Fig. S4). The result showed DNA synthesis to be inhibited in a UV dose-dependent manner. Under these reactions, ubiquitination of PCNA was similarly reduced and reached a level equivalent to that without dCTP on the template irradiated with the highest dose (1600 J/m^2), at which most of DNA synthesis was blocked just like that without dCTP (Supplementary Fig. S4a–c). By determining the status of PCNA mono-ubiquitination on UV-irradiated DNA by the method as shown in Fig. 4c, we concluded that the reduction of PCNA ubiquitination with UV-irradiated templates could be attributed to the reduced amounts of PCNA on DNA during elongation reactions (Supplementary Fig. S4d and e).

In the following experiments, we chose a template irradiated at 100 J/m^2, with which significant reduction of the full-length products was observed (Supplementary Fig. S4a). Since the lesions inhibited elongation with pol δ (Supplementary Fig. S4a), we could detect further elongation by addition of pol η when polymerase switching occurred.[49,50] After reactions in the presence of increasing amounts of pol η without RAD6A–RAD18, the products were analyzed by alkaline agarose gel electrophoresis (Fig. 5a). The results showed that the average size of the products was increased in a manner dependent on the amount of pol η up to 0.2 pmol (Fig. 5a, lanes 1–8 and graphs). However, further addition of excess pol η resulted in a decreased size of products, suggesting inhibitory effects on elongation (Fig. 5a, lanes 8–11 and graphs). When the template was replaced with intact mp18 DNA, inhibitory effects

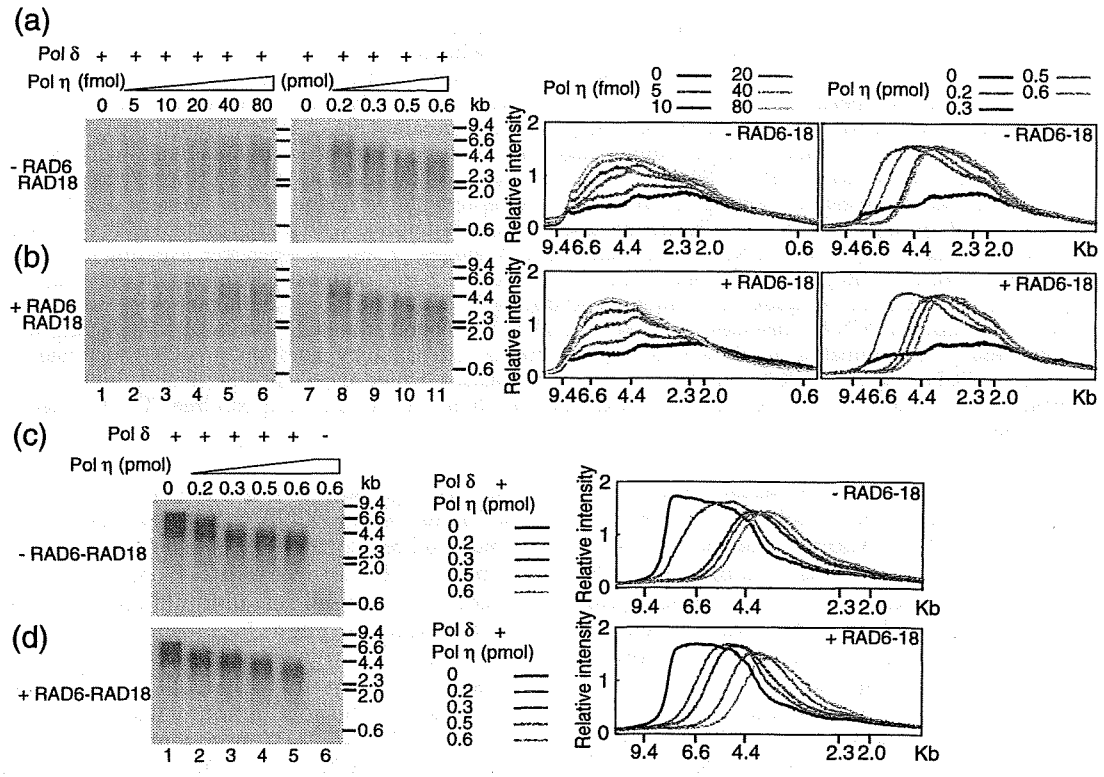

Fig. 5. Reconstitution of PCNA mono-ubiquitination-independent polymerase switching on UV-irradiated templates. Titration of pol η under standard reaction conditions containing RFs and UEs in the presence of pol δ (380 fmol). Intact (c and d) and UV-irradiated mp18 DNA (100 J/m^2) (a and b) were used as templates. Reactions were carried out for 10 min with the indicated amounts of pol η, in the presence (b and d) or absence (a and c) of RAD6A–RAD18. Products were analyzed by 0.7% alkaline agarose gel electrophoresis. The gel images were analyzed by Multi Gauge software (FUJIFILM), and the relative intensity of each lane is shown as a function of the product size in graphs.

on the elongation were also observed (Fig. 5c). By monitoring polymerase activity of pol η itself, we detected products around 0.6 kb with the maximum amount of pol η (Fig. 5c, lane 6), suggesting a much lower capacity for replication than with pol δ. We consider that the inhibition could be due to competitive association of pol η at 3′-ends. Such competition was not detected even when large amounts of pol β were introduced into the reaction mixture (Supplementary Fig. S5). These results indicated that pol η mechanistically has the potential to access 3′-ends without ubiquitination of PCNA and that polymerase switching between pol δ and pol η occurs frequently and spontaneously during DNA synthesis in this *in vitro* system.

Then, RAD6A–RAD18 was introduced to assess the effect of PCNA ubiquitination (Fig. 5b). The result showed that the size of products was also increased by addition of pol η, although we could not detect a clear difference from reactions without RAD6A–RAD18 using a wide range of concentrations of pol η (Fig. 5a and b). Furthermore, stimulation of pol η itself was also not clear (Fig. 5c and d, lane 6), which might be due to resolution of the products in this gel system. We considered the possibility that the concentration of template was sufficiently high for pol η to access 3′-ends without interaction with ubiquitinated PCNA.[51–53] To test this possibility, we reduced the concentration of the template as far as possible (Fig. 6). Again, the control

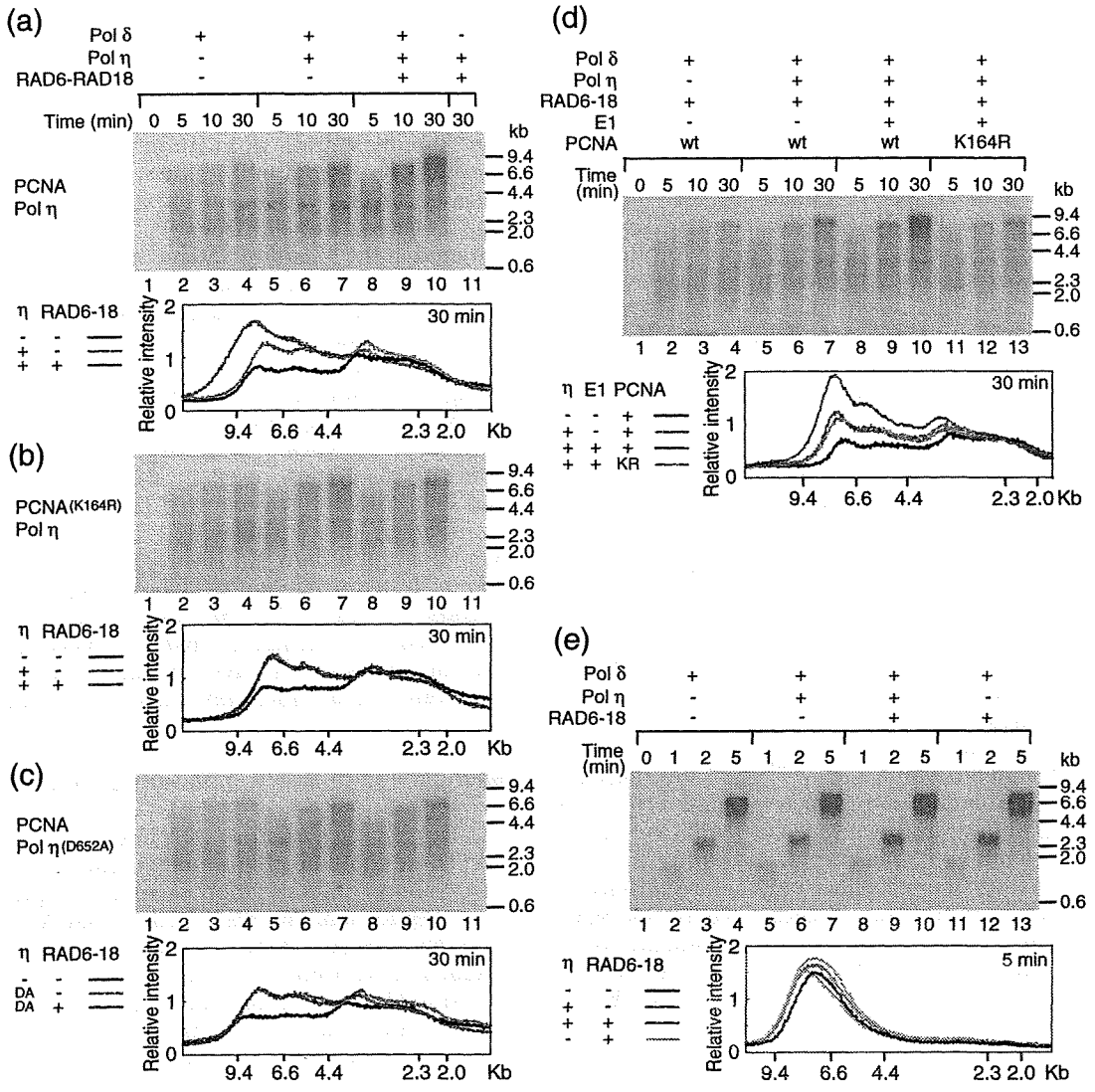

Fig. 6. Reconstitution of PCNA mono-ubiquitination-dependent polymerase switching on UV-irradiated templates. Intact (e) or UV-irradiated mp18 DNAs (100 J/m^2) (a–d) were used as templates. Reactions containing RFs, UEs, and indicated pols were carried out for the indicated times under the conditions described in Materials and Methods. For (b)–(d), wild-type proteins were replaced with the indicated mutants. Products were analyzed by 0.7% alkaline agarose gel electrophoresis. The gel images were analyzed by Multi Gauge software (FUJIFILM), and the relative intensity of each lane at 30 min (for UV-irradiated templates) or 5 min (for intact templates) is shown as a function of the product size in graphs.

reaction with pol δ alone showed a smear size distribution of the products, which was due to stalling of DNA replication (Fig. 6a, lanes 2–4 and graph). When pol η was introduced (Fig. 6a, lanes 5–7 and graph), an increase in the products (around 7 to 4 kb) was observed, demonstrating again ubiquitination-independent polymerase switching. Moreover, we now detected further accumulation of full-length products on addition of RAD6A–RAD18 (Fig. 6a, lanes 8–10 and graph). Under these reaction conditions, pol η seemed to be hardly contributing to gross DNA replication because no products were detectable after 30 min reaction with pol η in the absence of pol δ (Fig. 6a, lane 11). Notably, when the template was replaced with intact DNA, the replication finished after 5 min, and RAD6A–RAD18 and pol η were without effect (Fig. 6e).

It has been proposed that RAD6A–RAD18 has two biochemical functions for polymerase switching. One is mono-ubiquitination of PCNA. The other is targeting of pol η to 3′-ends by direct interaction.[6] To distinguish the respective contributions of the two functions of RAD6A–RAD18 in this *in vitro* system, we used a PCNA mutant, $PCNA^{(K164R)}$ (Fig. 6b). In the RAD6A–RAD18-independent reactions (Fig. 6b, lanes 5–7), an increase in the products of around 7 to 4 kb was observed to a similar extent as with wild-type PCNA (Fig. 6a). When RAD6A–RAD18 was introduced, no further accumulation of such products was observed (Fig. 6b, lanes 8–10 and graph). As a complementary experiment, E1 was omitted to prevent ubiquitination of PCNA in the presence of RAD6A–RAD18 (Fig. 6d). The results also demonstrated that omitting E1 (Fig. 6d, lanes 5–7) and replacement of PCNA with the mutant, $PCNA^{(K164R)}$ (Fig. 6d, lanes 11–13), reduced the amounts of such products to the same levels with each other, as compared with complete reactions (Fig. 6d, lanes 8–10 and graph). These results suggested that RAD6A–RAD18 itself could not stimulate recruitment of pol η without PCNA ubiquitination in this *in vitro* system.

To address the roles of UBZ[15] of pol η for polymerase switching, we replaced pol η with a UBZ defective mutant, pol $\eta^{(D652A)}$.[15] We detected clear accumulation of products around 7 to 4 kb with the mutant in the absence of RAD6A–RAD18 (Fig. 6c, lanes 5–7 and graph), indicating that the mutation did not affect either polymerase activity or the potential to access 3′-ends. When RAD6A–RAD18 was introduced, further accumulation of such products was not observed (Fig. 6c, lanes 8–10 and graph), demonstrating a crucial role of UBZ in stimulation of polymerase switching *in vitro*.

Discussion

In this work, we demonstrated that PCNA interacting with pol δ can act as a target for ubiquitination, and therefore, PCNA mono-ubiquitination could be coupled with DNA replication. Consequently, we could reconstitute replication-coupled switching between pol δ and pol η on a UV-irradiated template, while the results demonstrated discrepancies with currently accepted models, which have been proposed based on *in vivo* evidence, suggesting that regulatory factors could be missing in this *in vitro* system. Our results do allow us to discuss possible regulatory mechanisms of human pol switching.

Dynamic property of PCNA during the elongation phase of DNA synthesis

In this study, we demonstrated that PCNA accumulated on newly synthesized DNA during elongation. This is consistent with our previous report.[33] We have suggested that it could be a consequence of dynamic properties of pol δ previously.[33] Such a property of pol δ has been also described in other reports for mammalian[38,54] and yeast pol δ.[48,55] The general conclusion from these studies could be that pol δ is spontaneously and frequently dissociated from and associated to the 3′-ends during elongation. In our previous studies, we provided evidence that PCNA is released behind the 3′-end on such dissociation of pol δ. This is quite reasonable, because PCNA is tethered at the 3′-end by interactions with pol δ. We have also found that subsequent reloading of PCNA plays a crucial role in efficient elongation.[33] Therefore, it is rational and practical to attribute the accumulation of PCNA to its reloading during elongation. Notably, in yeast pol δ, accumulation of PCNA during DNA synthesis has been also reported.[48] However, several studies demonstrating opposite results also exist in the literature. Einolf and Guengerich have reported that processivity of mammalian pol δ calculated from kinetic parameters is quite high.[56] Recently, two studies have demonstrated stable pol δ–PCNA complexes at the 3′-ends in yeast.[57,58] The discrepancy might be attributed to a possibility that any modification(s) and/or accessory factor(s) in the respective preparations could differently affect the stability of pol δ.

Mechanisms of PCNA mono-ubiquitination

In this *in vitro* system, PCNA interacting with pol δ on DNA could be ubiquitinated efficiently so that PCNA mono-ubiquitination occurred coupled with DNA replication. In this reaction, RAD6–RAD18 probably accessed PCNA at the reverse side to the interaction with pol δ and RFC. This conclusion is supported by the finding that excess amounts of pol δ and RFC did not inhibit the ubiquitination reaction. Indeed, the Lys164 residue is found on the opposite side of the pol δ-interacting surface of PCNA.[59,60] A possible mechanism for the stimulation by pol δ and RFC could be that these proteins act to dispose PCNA on DNA with the proper geometry for catalysis. Indeed, it is known that the β-clamp of *E. coli*, the counterpart of PCNA, is tilted on DNA.[61] Tilted PCNA probably does not fit the catalytic site of RAD6–RAD18.

Our results showed that PCNA mono-ubiquitination is further stimulated by pol δ if the polymerase is actively replicating. This observation is consistent with findings in a cell-free system.[62] Importantly, the stimulation was not due to direct activation of ubiquitination reactions, but rather a consequence of multiple loading of PCNA molecules on the template, which was coupled with elongation.[33,48] Consequently, inhibition of elongation reduced the amounts of PCNA on the DNA, which also resulted in a decrease in the amount of ubiquitinated PCNA. Thus, growing 3′-ends and two conditions with stalled DNA synthesis, due to exhaustion of dNTP or DNA lesions, all appeared indistinguishable from one another in terms of biochemical actions of RFs, UEs, and pol δ. These findings indicate that factors that can recognize stalled replication itself and prevent association of RAD6A–RAD18 to moving replisome are missing in this *in vitro* system.

Mechanisms of polymerase switching

In this study, we reconstituted polymerase switching between pol δ and pol η, revealing two pathways *in vitro*. One is dependent on PCNA mono-ubiquitination and the other is independent of PCNA mono-ubiquitination, which predominates at higher concentrations of template DNA. This result suggested an intrinsic ability of pol η to access 3′-ends during replication, consistent with a previous report of a cell-free system.[63] Although our *in vitro* system revealed a mechanistic potential of pol η to access 3′-ends during replication, the PCNA mono-ubiquitination-independent pathway must be negligible *in vivo*, since genetic evidence has demonstrated the essential requirement of PCNA mono-ubiquitination for recruitment of pol η.[5,15,22,24,64,65] Importantly, Ouchida *et al.* have proposed the presence of a negative regulatory mechanism preventing inappropriate association of pol η with 3′-ends.[66] The discrepancy could be attributed to lack of protein factors involved in such a mechanism in this *in vitro* system.

The PCNA mono-ubiquitination-dependent reaction appeared at a very low concentration of 3′-end (130 pM, approximately 40 molecules/nucleus in human cells) and featured a crucial role for UBZ of pol η. The results suggest that interaction between UBZ and mono-ubiquitinated PCNA is essential for efficient bypass of one stalled 3′-end in the nucleus. Recent reports concerning yeast pol η in bypass reactions with mono-ubiquitinated PCNA have been contradictory. Polymerase activity of pol η was stimulated by mono-ubiquitinated PCNA in some but not all cases.[9,10] From our results, we consider that differences might be attributable to the assay conditions *in vitro*, depending on which of the two pathways is predominant.

Interaction between RAD6–RAD18 and pol η has been demonstrated,[6,12] and this might be responsible for recruitment to 3′-ends.[6] In the present study, however, polymerase switching was not stimulated by RAD6A–RAD18 itself when PCNA mono-ubiquitination was absent, suggesting that targeting of pol η by RAD6A–RAD18 could be coupled with PCNA ubiquitination.

Conceivable protein actions for human pol switching between pol δ and pol η in this *in vitro* system are shown in Fig. 7. The elongation complex consists of RFC, pol δ, and PCNA,[33] which could be a target for RAD6–RAD18. Usually, pol δ is not retained continuously at 3′-ends as a stable complex with PCNA; rather, it undergoes repeated association and dissociation cycles.[33,38,54] During this cycling,

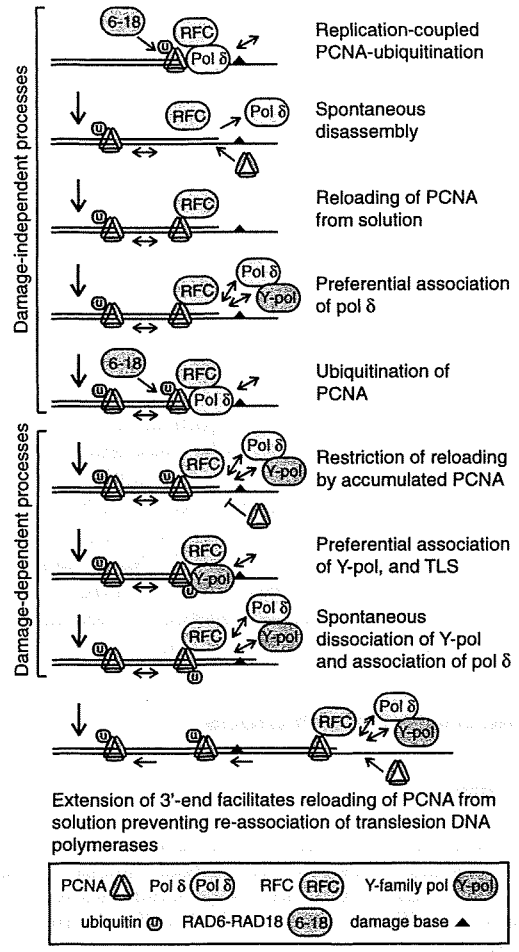

Fig. 7. Conceivable protein actions for PCNA mono-ubiquitination and polymerase switching in the present human *in vitro* system. The elongation complex consists of RFC, PCNA, and pol δ.[33] RAD6A–RAD18 preferentially ubiquitinates PCNA interacting with pol δ at a 3′-end. During association and dissociation cycles of pol δ in the growing 3′-end, the PCNA is released from the 3′-end of DNA, and new PCNA molecules are loaded from solution, preventing the pol η from association. At stalled 3′-ends, in contrast, PCNA accumulates and saturates on DNA during association and dissociation cycles of pol δ; consequently, the same PCNA molecules are repeatedly recruited to the 3′-end. Once the PCNA is ubiquitinated, it persists until association of pol η through interaction with the ubiquitinated PCNA. After DNA synthesis is restored, a fresh PCNA molecule is loaded from solution, reducing the probability of pol η access.

PCNA is released and left behind, and RFC incorporates PCNA that slides back to the 3′-end or reloads PCNA from solution.[33] These are dynamic and stochastic events. When PCNA molecules accumulate on DNA, the probability of reutilization is much higher than that of reloading from solution.[33] Thus, at growing ends, ubiquitin-free PCNA molecules normally tend to be loaded from solution. Under these circumstances, ubiquitinated PCNA molecules are not retained proximately to the 3′-ends so that pol η is restricted from association. At a stalled 3′-end, PCNA molecules are quickly accumulated onto DNA until reaching saturation. Consequently, the same PCNA molecule stays proximately to the stalled 3′-end. Once the PCNA molecule is ubiquitinated, it persists until pol η associates through interaction with the mono-ubiquitinated PCNA and extends the 3′-end. Once DNA synthesis is restored, PCNA molecules on DNA are diluted, facilitating reloading of fresh PCNA from solution and reducing the probability of pol η access.

Importantly, our results in the human system are quite different from some recent reports with a yeast system,[57,58] but not all.[48,55] In those reports,[57,58] it seems that pol δ is stably associated with PCNA during elongation but destabilizes with stalling replication. Such destabilization is more significant when PCNA is mono-ubiquitinated. Once pol η binds to ubiquitinated PCNA, association of pol δ is prohibited. Therefore, it is possible that some factors, which can stabilize pol δ–PCNA and pol η–PCNA interactions, could be missing in this human *in vitro* system.[33,37,38,54] Our system could thus be useful to address such missing factors for further understanding of molecular mechanisms of polymerase switching in humans.

Materials and Methods

Proteins

Recombinant human proteins were overproduced in *E. coli* cells and purified by conventional column chromatography. Detailed procedures for plasmid construction and protein purification are described in the Supplementary Data.

PCNA mono-ubiquitination assays

The standard reaction mixture (25 μl) contained 20 mM Hepes–NaOH (pH 7.5); 50 mM NaCl; 0.2 mg/ml bovine serum albumin (BSA); 1 mM DTT; 10 mM $MgCl_2$; 1 mM ATP; 0.1 mM each of dGTP, dATP, dCTP, and dTTP; 33 fmol of singly primed mp18 ssDNA (with the 90-mer primer, CTGCAAGGCGATTAAGTTGGGTAACGCCAGGGTTTTCCCAGTCACGACGTTGTAAAACGACGGCCAGTGCCAAGCTTGCATGCCTGCAGG); RPA (9 pmol); PCNA (1 pmol); RFC (88 fmol); E1 (850 fmol); RAD6A–RAD18 complex (950 fmol); and ubiquitin (170 pmol). Reaction mixtures were prepared on ice and then incubated at 30 °C for the indicated times. After termination of reactions with addition of 2 μl of 300 mM ethylenediaminetetraacetic acid (EDTA), the mixtures were immediately chilled on ice. Ubiquitination of PCNA was measured by Western analysis with an anti-PCNA antibody (Santa Cruz, sc-7907). Detection was carried out using an ECL chemiluminescence kit (GE Healthcare, Tokyo, Japan) and a CCD camera.

For ubiquitination assays with poly(dA)–oligo(dT), 100 ng of DNA including 900 fmol of oligo(dT) (GE Healthcare), instead of 33 fmol of mp18 DNA, was mixed under the standard reaction conditions except for the omission of dNTPs, RPA and RFC.

DNA replication assays

The standard reaction mixtures with [α-^{32}P]dTTP (25 μl) were preincubated at 30 °C for 1 min, and then reactions were started by addition of pol δ (380 fmol). After incubation at 30 °C for the indicated times, reactions were terminated with 2 μl of 300 mM EDTA, and the mixtures were immediately chilled on ice. Products of DNA synthesis were analyzed as described earlier.[33] Gel images of autoradiography were analyzed by Multi Gauge software Version 3.0 (FUJIFILM, Tokyo, Japan).

For replication assays with poly(dA)–oligo(dT), 100 ng of DNA including 900 fmol of oligo(dT) (GE Healthcare), instead of 33 fmol of mp18 DNA, was mixed under the standard reaction conditions including [α-^{32}P]dTTP, but not other dNTPs, RPA and RFC.

PCNA mono-ubiquitination of DNA–PCNA complexes isolated by gel filtration

For the introduction of nicks, plasmid pUC18 was reacted with N.BstNBI (New England BioLabs, Tokyo, Japan) at 55 °C for 60 min. Then, DNA was extracted with phenol/chloroform and precipitated with ethanol. PCNA (8 pmol), RFC$^{(p140N555)}$ (36 fmol), and the nicked plasmid pUC18 (133 fmol) were incubated at 30 °C for 15 min in 100 μl of buffer containing 20 mM Hepes–NaOH (pH 7.5), 100 mM NaCl, 0.2 mg/ml BSA, 1 mM DTT, 10 mM $MgCl_2$, and 1 mM ATP. The mixture was then immediately applied at room temperature to a 2-ml column of 4% agarose beads (A-1040-S, Agarose Beads Technologies, Madrid, Spain) equilibrated in buffer containing 20 mM Hepes–NaOH (pH 7.5), 1 mM DTT, 10 mM $MgCl_2$, and 50 mM NaCl, and fractions of three drops each were collected on ice. The fractions eluted in void volume containing DNA were pooled, and then 12.5-μl aliquots were incubated with E1 (850 fmol), RAD6A–RAD18 complex (38 fmol), and ubiquitin (170 pmol) in the presence of the indicated amounts of RFC or pol δ at 30 °C for 30 min in 25-μl reaction mixtures [20 mM Hepes–NaOH (pH 7.5), 50 mM NaCl, 0.2 mg/ml BSA, 1 mM DTT, 10 mM $MgCl_2$, 1 mM ATP, and 0.1 mM each of dGTP, dATP, and dTTP].

Isolation of PCNA on DNA bound to magnetic beads

The 5′-biotinylated primer (TCTCTCTCTCTGCAAGGCGATTAAGTTGGGTAACGCCAGGGTTTTCCCAGTCACGACGTTGTAAAACGACGGCCAGTGCCAAGCTTGCATGCCTGCAGG) was annealed to 33 fmol mp18 ssDNA and immobilized onto a 10-μl suspension of streptavidin magnetic beads, Dynabeads M280 (Life Technologies, Tokyo, Japan), as described previously.[33] Assays were carried out under standard reaction conditions as described for Fig. 4c. After termination of the reactions with 2 μl of 300 mM EDTA, the beads were washed and analyzed.[33]

Assay for PCNA mono-ubiquitination-dependent polymerase switching

RPA (900 fmol), PCNA (1 pmol), RFC (26 fmol), E1 (850 fmol), RAD6A–RAD18 complex (950 fmol), ubiquitin (170 pmol), and 3.3 fmol of singly primed mp18 ssDNA (with the 36-mer primer, CAGGGTTTTCCCAGTCACGACGTTGTAAAACGACGG) were mixed under standard reaction conditions with [α-^{32}P]dTTP in the presence or absence of pol η (10 fmol). After incubation at 30 °C for 1 min, pol δ (750 fmol) was added and the mixture was further incubated for the indicated times. Reaction products (10 μl) were analyzed by 0.7% alkaline agarose gel electrophoresis.[33] Gel images of autoradiography were analyzed by Multi Gauge software Version 3.0 (FUJIFILM).

Acknowledgements

We thank Dr. Marc S. Wold (University of Iowa College of Medicine, Iowa City, IA), Dr. Fumio Hanaoka (Osaka University, Osaka, Japan), Dr. Toshiki Tsurimoto (Kyushu University, Fukuoka, Japan), Dr. Tomohiko Ohta (St. Marianna University School of Medicine, Kanagawa, Japan), and Dr. Tadashi Shimamoto (Hiroshima University, Hiroshima, Japan) for respectively providing an RPA expression plasmid, *POLH* cDNA, a PCNA expression plasmid, a ubiquitin-encoding plasmid, and an *E. coli* strain to produce mp18 ssDNA. Several cloning vectors were obtained from the National BioResource Project (National Institute of Genetics, Japan). We also thank Dr. Niels de Wind (Leiden University Medical Center, Leiden, The Netherlands) and Dr. Hiroshi Hashimoto (Yokohama City University, Kanagawa) for their comments and suggestions on the manuscript. We are grateful to Kenji Masuda for his help with cDNA cloning and Tomoka Nakashima, Fumie Okubo, Kazumi Shimamoto, Miki Suzuki, and Mai Yoshida for their laboratory assistance. This work was supported by Grants-in-Aid from the Ministry of Education, Culture, Sports, Science and Technology of Japan (to Y.M. and K.K.); by the 21st Century Center of Excellence program from the Ministry of Education, Culture, Sports, Science and Technology of Japan (to K.K.); by Health and Labour Science Research Grants (to K.K.); by Grants-in-Aid for Cancer Research from the Ministry of Health, Labour and Welfare (to K.K.); and by the Radiation Effects Association (to Y.M.). During the performance of this work, J.P. was supported by a Japan Society for the Promotion of Science Research Fellowship for Young Scientists.

Supplementary Data

Supplementary data associated with this article can be found, in the online version, at doi:10.1016/j.jmb.2010.01.003

References

1. Hishida, T., Kubota, Y., Carr, A. M. & Iwasaki, H. (2009). *RAD6–RAD18–RAD5*-pathway-dependent tolerance to chronic low-dose ultraviolet light. *Nature*, **457**, 612–615.
2. Lehmann, A. R., Niimi, A., Ogi, T., Brown, S., Sabbioneda, S., Wing, J. F. *et al.* (2007). Translesion synthesis: Y-family polymerases and the polymerase switch. *DNA Repair (Amst.)*, **6**, 891–899.
3. Andersen, P. L., Xu, F. & Xiao, W. (2008). Eukaryotic DNA damage tolerance and translesion synthesis through covalent modifications of PCNA. *Cell Res.* **18**, 162–173.
4. Hoege, C., Pfander, B., Moldovan, G. L., Pyrowolakis, G. & Jentsch, S. (2002). RAD6-dependent DNA repair is linked to modification of PCNA by ubiquitin and SUMO. *Nature*, **419**, 135–141.
5. Stelter, P. & Ulrich, H. D. (2003). Control of spontaneous and damage-induced mutagenesis by SUMO and ubiquitin conjugation. *Nature*, **425**, 188–191.
6. Watanabe, K., Tateishi, S., Kawasuji, M., Tsurimoto, T., Inoue, H. & Yamaizumi, M. (2004). Rad18 guides polη to replication stalling sites through physical interaction and PCNA monoubiquitination. *EMBO J.* **23**, 3886–3896.
7. Bailly, V., Lamb, J., Sung, P., Prakash, S. & Prakash, L. (1994). Specific complex formation between yeast RAD6 and RAD18 proteins: a potential mechanism for targeting RAD6 ubiquitin-conjugating activity to DNA damage sites. *Genes Dev.* **8**, 811–820.
8. Bailly, V., Lauder, S., Prakash, S. & Prakash, L. (1997). Yeast DNA repair proteins Rad6 and Rad18 form a heterodimer that has ubiquitin conjugating, DNA binding, and ATP hydrolytic activities. *J. Biol. Chem.* **272**, 23360–23365.
9. Garg, P. & Burgers, P. M. (2005). Ubiquitinated proliferating cell nuclear antigen activates translesion DNA polymerases η and REV1. *Proc. Natl Acad. Sci. USA*, **102**, 18361–18366.
10. Haracska, L., Unk, I., Prakash, L. & Prakash, S. (2006). Ubiquitylation of yeast proliferating cell nuclear antigen and its implications for translesion DNA synthesis. *Proc. Natl Acad. Sci. USA*, **103**, 6477–6482.
11. Xin, H., Lin, W., Sumanasekera, W., Zhang, Y., Wu, X. & Wang, Z. (2000). The human *RAD18* gene product interacts with HHR6A and HHR6B. *Nucleic Acids Res.* **28**, 2847–2854.
12. Yuasa, M. S., Masutani, C., Hirano, A., Cohn, M. A., Yamaizumi, M., Nakatani, Y. & Hanaoka, F. (2006). A human DNA polymerase η complex containing Rad18, Rad6 and Rev1; proteomic analysis and targeting of the complex to the chromatin-bound fraction of cells undergoing replication fork arrest. *Genes Cells*, **11**, 731–744.
13. Unk, I., Hajdu, I., Fatyol, K., Szakal, B., Blastyak, A., Bermudez, V. *et al.* (2006). Human SHPRH is a ubiquitin ligase for Mms2-Ubc13-dependent polyubiquitylation of proliferating cell nuclear antigen. *Proc. Natl Acad. Sci. USA*, **103**, 18107–18112.
14. Bi, X., Barkley, L. R., Slater, D. M., Tateishi, S., Yamaizumi, M., Ohmori, H. & Vaziri, C. (2006). Rad18 regulates DNA polymerase κ and is required for recovery from S-phase checkpoint-mediated arrest. *Mol. Cell. Biol.* **26**, 3527–3540.
15. Bienko, M., Green, C. M., Crosetto, N., Rudolf, F., Zapart, G., Coull, B. *et al.* (2005). Ubiquitin-binding domains in Y-family polymerases regulate translesion synthesis. *Science*, **310**, 1821–1824.

16. Guo, C., Tang, T. S., Bienko, M., Parker, J. L., Bielen, A. B., Sonoda, E. *et al.* (2006). Ubiquitin-binding motifs in REV1 protein are required for its role in the tolerance of DNA damage. *Mol. Cell. Biol.* **26**, 8892–8900.
17. Kannouche, P. L., Wing, J. & Lehmann, A. R. (2004). Interaction of human DNA polymerase η with monoubiquitinated PCNA: a possible mechanism for the polymerase switch in response to DNA damage. *Mol. Cell*, **14**, 491–500.
18. Plosky, B. S., Vidal, A. E., Fernandez de Henestrosa, A. R., McLenigan, M. P., McDonald, J. P., Mead, S. & Woodgate, R. (2006). Controlling the subcellular localization of DNA polymerases ι and η via interactions with ubiquitin. *EMBO J.* **25**, 2847–2855.
19. Motegi, A., Sood, R., Moinova, H., Markowitz, S. D., Liu, P. P. & Myung, K. (2006). Human SHPRH suppresses genomic instability through proliferating cell nuclear antigen polyubiquitination. *J. Cell Biol.* **175**, 703–708.
20. Motegi, A., Liaw, H. J., Lee, K. Y., Roest, H. P., Maas, A., Wu, X. *et al.* (2008). Polyubiquitination of proliferating cell nuclear antigen by HLTF and SHPRH prevents genomic instability from stalled replication forks. *Proc. Natl Acad. Sci. USA*, **105**, 12411–12416.
21. Unk, I., Hajdu, I., Fatyol, K., Hurwitz, J., Yoon, J. H., Prakash, L. *et al.* (2008). Human HLTF functions as a ubiquitin ligase for proliferating cell nuclear antigen polyubiquitination. *Proc. Natl Acad. Sci. USA*, **105**, 3768–3773.
22. Arakawa, H., Moldovan, G. L., Saribasak, H., Saribasak, N. N., Jentsch, S. & Buerstedde, J. M. (2006). A role for PCNA ubiquitination in immunoglobulin hypermutation. *PLoS Biol.* **4**, e366.
23. Edmunds, C. E., Simpson, L. J. & Sale, J. E. (2008). PCNA ubiquitination and REV1 define temporally distinct mechanisms for controlling translesion synthesis in the avian cell line DT40. *Mol. Cell*, **30**, 519–529.
24. Langerak, P., Nygren, A. O., Krijger, P. H., van den Berk, P. C. & Jacobs, H. (2007). A/T mutagenesis in hypermutated immunoglobulin genes strongly depends on $PCNA^{K164}$ modification. *J. Exp. Med.* **204**, 1989–1998.
25. Delbos, F., De Smet, A., Faili, A., Aoufouchi, S., Weill, J. C. & Reynaud, C. A. (2005). Contribution of DNA polymerase η to immunoglobulin gene hypermutation in the mouse. *J. Exp. Med.* **201**, 1191–1196.
26. Martomo, S. A., Yang, W. W., Wersto, R. P., Ohkumo, T., Kondo, Y., Yokoi, M. *et al.* (2005). Different mutation signatures in DNA polymerase η- and MSH6-deficient mice suggest separate roles in antibody diversification. *Proc. Natl Acad. Sci. USA*, **102**, 8656–8661.
27. Zeng, X., Winter, D. B., Kasmer, C., Kraemer, K. H., Lehmann, A. R. & Gearhart, P. J. (2001). DNA polymerase η is an A–T mutator in somatic hypermutation of immunoglobulin variable genes. *Nat. Immunol.* **2**, 537–541.
28. Frampton, J., Irmisch, A., Green, C. M., Neiss, A., Trickey, M., Ulrich, H. D. *et al.* (2006). Postreplication repair and PCNA modification in *Schizosaccharomyces pombe*. *Mol. Biol. Cell*, **17**, 2976–2985.
29. Simpson, L. J., Ross, A. L., Szuts, D., Alviani, C. A., Oestergaard, V. H., Patel, K. J. & Sale, J. E. (2006). RAD18-independent ubiquitination of proliferating-cell nuclear antigen in the avian cell line DT40. *EMBO Rep.* **7**, 927–932.
30. Huang, T. T., Nijman, S. M., Mirchandani, K. D., Galardy, P. J., Cohn, M. A., Haas, W. *et al.* (2006). Regulation of monoubiquitinated PCNA by DUB autocleavage. *Nat. Cell Biol.* **8**, 339–347.
31. Oestergaard, V. H., Langevin, F., Kuiken, H. J., Pace, P., Niedzwiedz, W., Simpson, L. J. *et al.* (2007). Deubiquitination of FANCD2 is required for DNA crosslink repair. *Mol. Cell*, **28**, 798–809.
32. Davies, A. A., Huttner, D., Daigaku, Y., Chen, S. & Ulrich, H. D. (2008). Activation of ubiquitin-dependent DNA damage bypass is mediated by replication protein A. *Mol. Cell*, **29**, 625–636.
33. Masuda, Y., Suzuki, M., Piao, J., Gu, Y., Tsurimoto, T. & Kamiya, K. (2007). Dynamics of human replication factors in the elongation phase of DNA replication. *Nucleic Acids Res.* **35**, 6904–6916.
34. Zuo, S., Bermudez, V., Zhang, G., Kelman, Z. & Hurwitz, J. (2000). Structure and activity associated with multiple forms of *Schizosaccharomyces pombe* DNA polymerase δ. *J. Biol. Chem.* **275**, 5153–5162.
35. Burgers, P. M. & Gerik, K. J. (1998). Structure and processivity of two forms of *Saccharomyces cerevisiae* DNA polymerase δ. *J. Biol. Chem.* **273**, 19756–19762.
36. Lee, M. Y., Tan, C. K., Downey, K. M. & So, A. G. (1984). Further studies on calf thymus DNA polymerase δ purified to homogeneity by a new procedure. *Biochemistry*, **23**, 1906–1913.
37. Podust, L. M., Podust, V. N., Sogo, J. M. & Hübscher, U. (1995). Mammalian DNA polymerase auxiliary proteins: analysis of replication factor C-catalyzed proliferating cell nuclear antigen loading onto circular double-stranded DNA. *Mol. Cell. Biol.* **15**, 3072–3081.
38. Podust, V. N., Chang, L. S., Ott, R., Dianov, G. L. & Fanning, E. (2002). Reconstitution of human DNA polymerase δ using recombinant baculoviruses: the p12 subunit potentiates DNA polymerizing activity of the four-subunit enzyme. *J. Biol. Chem.* **277**, 3894–3901.
39. Tsurimoto, T. & Stillman, B. (1991). Replication factors required for SV40 DNA replication *in vitro*. I. DNA structure-specific recognition of a primer-template junction by eukaryotic DNA polymerases and their accessory proteins. *J. Biol. Chem.* **266**, 1950–1960.
40. Fukuda, K., Morioka, H., Imajou, S., Ikeda, S., Ohtsuka, E. & Tsurimoto, T. (1995). Structure–function relationship of the eukaryotic DNA replication factor, proliferating cell nuclear antigen. *J. Biol. Chem.* **270**, 22527–22534.
41. Tsurimoto, T., Shinozaki, A., Yano, M., Seki, M. & Enomoto, T. (2005). Human Werner helicase interacting protein 1 (WRNIP1) functions as a novel modulator for DNA polymerase δ. *Genes Cells*, **10**, 13–22.
42. Shikata, K., Ohta, S., Yamada, K., Obuse, C., Yoshikawa, H. & Tsurimoto, T. (2001). The human homologue of fission Yeast cdc27, p66, is a component of active human DNA polymerase δ. *J. Biochem.* **129**, 699–708.
43. Burgers, P. M. & Yoder, B. L. (1993). ATP-independent loading of the proliferating cell nuclear antigen requires DNA ends. *J. Biol. Chem.* **268**, 19923–19926.
44. Uhlmann, F., Cai, J., Gibbs, E., O'Donnell, M. & Hurwitz, J. (1997). Deletion analysis of the large subunit p140 in human replication factor C reveals regions required for complex formation and replication activities. *J. Biol. Chem.* **272**, 10058–10064.
45. Podust, V. N., Tiwari, N., Stephan, S. & Fanning, E. (1998). Replication factor C disengages from proliferating cell nuclear antigen (PCNA) upon sliding clamp formation, and PCNA itself tethers DNA polymerase δ to DNA. *J. Biol. Chem.* **273**, 31992–31999.

46. Yao, N., Turner, J., Kelman, Z., Stukenberg, P. T., Dean, F., Shechter, D. *et al.* (1996). Clamp loading, unloading and intrinsic stability of the PCNA, β and gp45 sliding clamps of human, *E. coli* and T4 replicases. *Genes Cells*, **1**, 101–113.
47. Yuzhakov, A., Kelman, Z., Hurwitz, J. & O'Donnell, M. (1999). Multiple competition reactions for RPA order the assembly of the DNA polymerase δ holoenzyme. *EMBO J.* **18**, 6189–6199.
48. Chilkova, O., Stenlund, P., Isoz, I., Stith, C. M., Grabowski, P., Lundstrom, E. B. *et al.* (2007). The eukaryotic leading and lagging strand DNA polymerases are loaded onto primer-ends via separate mechanisms but have comparable processivity in the presence of PCNA. *Nucleic Acids Res.* **35**, 6588–6597.
49. Masutani, C., Kusumoto, R., Yamada, A., Dohmae, N., Yokoi, M., Yuasa, M. *et al.* (1999). The *XPV* (xeroderma pigmentosum variant) gene encodes human DNA polymerase η. *Nature*, **399**, 700–704.
50. Masutani, C., Araki, M., Yamada, A., Kusumoto, R., Nogimori, T., Maekawa, T. *et al.* (1999). Xeroderma pigmentosum variant (XP-V) correcting protein from HeLa cells has a thymine dimer bypass DNA polymerase activity. *EMBO J.* **18**, 3491–3501.
51. Haracska, L., Johnson, R. E., Unk, I., Phillips, B., Hurwitz, J., Prakash, L. & Prakash, S. (2001). Physical and functional interactions of human DNA polymerase η with PCNA. *Mol. Cell. Biol.* **21**, 7199–7206.
52. Haracska, L., Kondratick, C. M., Unk, I., Prakash, S. & Prakash, L. (2001). Interaction with PCNA is essential for yeast DNA polymerase η function. *Mol. Cell*, **8**, 407–415.
53. Kusumoto, R., Masutani, C., Shimmyo, S., Iwai, S. & Hanaoka, F. (2004). DNA binding properties of human DNA polymerase η: implications for fidelity and polymerase switching of translesion synthesis. *Genes Cells*, **9**, 1139–1150.
54. Tsurimoto, T. & Stillman, B. (1989). Multiple replication factors augment DNA synthesis by the two eukaryotic DNA polymerases, α and δ. *EMBO J.* **8**, 3883–3889.
55. McCulloch, S. D., Kokoska, R. J., Garg, P., Burgers, P. M. & Kunkel, T. A. (2009). The efficiency and fidelity of 8-oxo-guanine bypass by DNA polymerases δ and η. *Nucleic Acids Res.* **37**, 2830–2840.
56. Einolf, H. J. & Guengerich, F. P. (2000). Kinetic analysis of nucleotide incorporation by mammalian DNA polymerase δ. *J. Biol. Chem.* **275**, 16316–16322.
57. Langston, L. D. & O'Donnell, M. (2008). DNA polymerase δ is highly processive with proliferating cell nuclear antigen and undergoes collision release upon completing DNA. *J. Biol. Chem.* **283**, 29522–29531.
58. Zhuang, Z., Johnson, R. E., Haracska, L., Prakash, L., Prakash, S. & Benkovic, S. J. (2008). Regulation of polymerase exchange between Polη and Polδ by monoubiquitination of PCNA and the movement of DNA polymerase holoenzyme. *Proc. Natl Acad. Sci. USA*, **105**, 5361–5366.
59. Gulbis, J. M., Kelman, Z., Hurwitz, J., O'Donnell, M. & Kuriyan, J. (1996). Structure of the C-terminal region of p21(WAF1/CIP1) complexed with human PCNA. *Cell*, **87**, 297–306.
60. Jonsson, Z. O., Hindges, R. & Hübscher, U. (1998). Regulation of DNA replication and repair proteins through interaction with the front side of proliferating cell nuclear antigen. *EMBO J.* **17**, 2412–2425.
61. Georgescu, R. E., Kim, S. S., Yurieva, O., Kuriyan, J., Kong, X. P. & O'Donnell, M. (2008). Structure of a sliding clamp on DNA. *Cell*, **132**, 43–54.
62. Schmutz, V., Wagner, J., Janel-Bintz, R., Fuchs, R. P. & Cordonnier, A. M. (2007). Requirements for PCNA monoubiquitination in human cell-free extracts. *DNA Repair (Amst.)*, **6**, 1726–1731.
63. Bebenek, K., Matsuda, T., Masutani, C., Hanaoka, F. & Kunkel, T. A. (2001). Proofreading of DNA polymerase η-dependent replication errors. *J. Biol. Chem.* **276**, 2317–2320.
64. Acharya, N., Yoon, J. H., Gali, H., Unk, I., Haracska, L., Johnson, R. E. *et al.* (2008). Roles of PCNA-binding and ubiquitin-binding domains in human DNA polymerase η in translesion DNA synthesis. *Proc. Natl Acad. Sci. USA*, **105**, 17724–17729.
65. Parker, J. L., Bielen, A. B., Dikic, I. & Ulrich, H. D. (2007). Contributions of ubiquitin- and PCNA-binding domains to the activity of polymerase η in *Saccharomyces cerevisiae*. *Nucleic Acids Res.* **35**, 881–889.
66. Ouchida, R., Ukai, A., Mori, H., Kawamura, K., Dolle, M. E., Tagawa, M. *et al.* (2008). Genetic analysis reveals an intrinsic property of the germinal center B cells to generate A:T mutations. *DNA Repair (Amst.)*, **7**, 1392–1398.

Biochemical and Biophysical Research Communications 392 (2010) 140–144

Contents lists available at ScienceDirect

Biochemical and Biophysical Research Communications

journal homepage: www.elsevier.com/locate/ybbrc

Specific amino acid residues are involved in substrate discrimination and template binding of human REV1 protein

Jinlian Piao, Yuji Masuda *, Kenji Kamiya *

Research Institute for Radiation Biology and Medicine, Hiroshima University, 1-2-3 Kasumi, Minami-ku, Hiroshima 734-8553, Japan

ARTICLE INFO

Article history:
Received 9 December 2009
Available online 6 January 2010

Keywords:
Y-family DNA polymerase
Deoxycytidyl transferase
Kinetic parameter

ABSTRACT

REV1 is a member of the Y-family DNA polymerases, but is atypical in utilizing only dCTP with a preference for guanine (G) as the template. Crystallography of the REV1–DNA–dCTP ternary complex has revealed a unique mechanism by which template G is evicted from the DNA helix and incoming dCTP is recognized by an arginine residue in an α-loop, termed the N-digit. To better understand functions of its individual amino acid residues, we made a series of mutant human REV1 proteins. We found that R357 and L358 play vital roles in template binding. Furthermore, extensive mutation analysis revealed a novel function of R357 for substrate discrimination, in addition to previously proposed specific interaction with incoming dCTP. We found that the binding pocket for dCTP of REV1 has also significant but latent affinity for dGTP. The results suggest that the positive charge on R357 could prevent interaction with dGTP. We propose that both direct and indirect mechanisms mediated by R357 ensure specificity for dCTP.

Introduction

Accurate DNA replication is crucial for living organisms. Replicases, which are responsible for genomic duplication, are high-fidelity DNA polymerases whose fidelity is achieved by two characteristics [1]. One is high nucleotide selectivity. The correct Watson–Crick base pair is able to enter into binding pockets without steric clashes. The other is proof reading activity catalyzed by intrinsic 3′ exonuclease. As a consequence of these properties, replicases can not extend primer termini beyond damage bases, resulting in replication blocks [1].

Cells also have another class of DNA polymerases [2], the Y-family members pol η, ι, and κ, which are able to extend primer ends beyond damage bases [3,4]. Consequently, stalled DNA synthesis can be restored. The molecular mechanism allowing incorporation of a deoxyribonucleotide opposite a damaged template is of great interest and there is evidence that a lack of proofreading activity and lower nucleotide selectivity are involved [1], even though DNA polymerase η an κ also utilize Watson–Crick base pairs for nucleotide selection [4]. DNA polymerase ι has an additional property, which is utilization of Hoogsteen base pairs for nucleotide selection, to bypass damage bases [4].

REV1 is a well-conserved Y-family polymerase in eukaryotes. Despite belonging with polymerase family, this enzyme is able to utilize only dCTP as the dNTP source for its deoxycytidyl transferase activity [5]. dCMP is thereby incorporated opposite template G, various DNA lesions, and also opposite templates A, T, and C [6]. Steady-state kinetic studies have demonstrated that templates G and apurinic/apyrimidinic (AP) site are good substrates for the transferase reactions [7–10] and crystallography of yeast and human REV1 has revealed unique mechanisms for recognition of template G and incoming dCTP [11,12]. REV1 has a loose α-loop structure, termed the N-digit, and another structure, named the G-loop, which are conserved in the REV1 family, but not other Y polymerase members. The template G and incoming dCTP do not pair with each other. Instead, the template G is evicted from the DNA helix and interacts with amino acids in the G-loop, and incoming dCTP forms a hydrogen bond with an arginine residue in the N-digit [11,12].

In the present study, we made a series of mutant human REV1 proteins to analyse which amino acid residues are involved in substrate discrimination and template binding. The results suggested that the conserved amino acid residues in the N-digit play crucial roles in bypass synthesis of damaged templates. Together with information from the crystal structure, we discuss novel functions of the N-digit for substrate discrimination and template binding of human REV1 protein.

Abbreviations: AP, apurinic/apyrimidinic; F, tetrahydrofuran; 8oxG, 8-oxoguanine.

* Corresponding authors. Fax: +81 82 257 5843 (Y. Masuda); +81 82 257 5844 (K. Kamiya).

E-mail addresses: piao@hiroshima-u.ac.jp (J. Piao), masudayu@hiroshima-u.ac.jp (Y. Masuda), kkamiya@hiroshima-u.ac.jp (K. Kamiya).

0006-291X/$ - see front matter © 2010 Elsevier Inc. All rights reserved.
doi:10.1016/j.bbrc.2009.12.167

Materials and methods

Proteins. Truncated human *REV1* genes were made by PCR with introduction of an NdeI site at the initiation codon, and inserted into the NdeI site of pET15b. In some cases, the coding region of the resulting plasmids was subcloned into an XbaI site of pBAD22A in which gene expression was induced by arabinose [13]. All proteins were purified as his-tagged fusion proteins, as described previously [13,14] by sequential chromatography using HiTrap Chelating and Superdex 200 columns (GE Healthcare). Protein concentrations were determined by BIO-RAD protein assay using BSA (BIO-RAD) as the standard.

Transferase assay. Oligonucleotide templates 5′-CTCGTCAGCAT CTTCAXCATACAGTCAGTG-3′ [X = G, A, T, C, tetrahydrofuran (F) and 8-oxoguanine (8oxG)] and the primer 5′-CACTGACTGTATG-3′ were purchased. The latter was labeled using polynucleotide kinase (New England BioLabs) and [γ-^{32}P] ATP (GE Healthcare), and annealed to the templates. The standard reaction mixture (25 μl) contained 50 mM Tris–HCl buffer, pH 8.0, 2 mM $MgCl_2$, 25 mM $(NH_4)_2SO_4$, 0.1 mg/ml BSA, 5 mM dithiothreitol, 0.1 mM dNTP, 100 nM primer-template and 1 μl of protein sample, diluted with buffer (50 mM HEPES [4-(2-hydroxyethyl)-1-piperazineethanesulfonic acid]–NaOH, pH 7.5, 10% glycerol, 10 mM β-mercaptoethanol, 500 mM NaCl, and 0.1 mg/ml BSA) as indicated. After incubation at 30 °C for the indicated time, reactions were terminated with 10 μl of stop solution (30 mM EDTA/94% formamide/0.05% bromophenol blue/0.05% xylene cyanole) and products were resolved on 20% polyacrylamide gels containing 8 M urea and autoradiographed at −80 °C. The amount of DNA present in each band was quantified using a Bio-Imaging Analyzer BAS2000 (Fuji Photo Film Co., Ltd.).

Results

To determine the minimum region required for the deoxycytidyl transferase activity of REV1 protein, we made and purified a series of deletion mutants as his-tagged fusion proteins at the N-termini. The transferase activities of the truncated proteins were measured by the standard assay containing 0.1 mM dCTP and 100 nM primer-template with template G. The results revealed that the minimum region exhibiting equivalent activity with full length REV1 was the portion between amino acid residues 341 and 829 (Fig. 1A). Further truncation of 29 amino acid residues at the N-terminal or 10 amino acid residues at the C-terminal reduced the transferase activity to less than 1% of the wild-type value. The kinetic parameters of the deletion mutant consisting of the minimum region, REV1$^{(341–829)}$ indicated that the activity was in fact slightly higher than that of the full-length protein (Table 1). We considered that the difference is due to the instability of the full-length protein [13] but the properties were found to be essentially identical (Table 1). We concluded that the REV1$^{(341–829)}$ is the necessary and sufficient region for the transferase activity, which is slightly shorter than that previously reported [12].

The N-terminal 29 amino acid residues of REV1$^{(341–829)}$, which is the portion of the α-helix structure named the N-digit [12], proved essential for transferase activity (Fig. 1A). The region is well conserved in REV1 proteins of various species (Fig. 1B). To determine the functional role of the conserved amino acid residues, we first replaced each of the most conserved five amino acid residues of REV1$^{(341–829)}$ with alanines (Fig. 1B). The mutant proteins F348A, S356A, R357A, L358A, and H359A were produced in *E. coli*, and purified with the same qualities (Fig. 2).

Then, we determined kinetic parameters of these mutants using template G, and 8oxG and F as model substrates for damaged bases. The replacement of F348 with alanine did not greatly affect the dCMP transferase activity (Table 2). In contrast, replacements in the conserved SRLH motif markedly reduced the activity

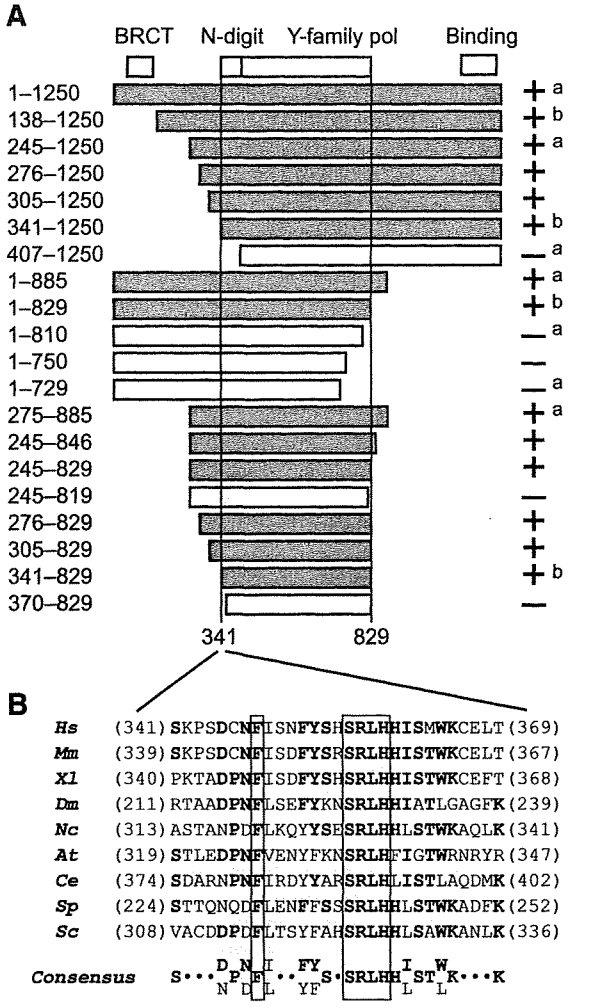

Fig. 1. Deletion analysis of human REV1 protein. (A) Schematic representation of deletion mutants of REV1 protein with their activities. Numbers indicate corresponding amino acid residues of deletion mutants. BRCT, BRCA1 C terminal (BRCT) domain; Y-family pol, conserved region among the family. Binding, binding domain with REV7 and other Y-family DNA polymerases, polη, ι, and κ. + and gray boxes represent activity more than 50% of the full length level. – and open boxes represent transferase activity less than 1% of the full length level. a, data from Ref. [13]. b, data from Ref. [14]. (B) Alignment of amino acid sequences between 341–369 of human REV1 (*Hs*) and corresponding regions of *Mm* (*Mus musculus*), *Xl* (*Xenopus laevis*), *Dm* (*Drosophila melanogaster*), *Nc* (*Neurospora crassa*), *At* (*Arabidopsis thaliana*), *Ce* (*Caenorhabditis elegans*), *Sp* (*Schizosaccharomyces pombe*), and *Sc* (*Saccharomyces cerevisiae*). The conserved amino acids residues are shown in bold letters and the most conserved ones are boxed.

(Table 2). In particular, replacement of R357 and L358 strongly reduced k_{cat} and increased K_M values with the three templates (Table 2). To test the possibility that the defect might be attributed, at least in part, to lowered affinities to template DNA, we determined K_M values. Expectedly, the result showed that K_M values for the three templates with these mutants were much higher than that for wild-type (Table 3), suggesting vital roles of R357 and L358 residues in DNA binding. Interestingly, with L358A the defects in template G and template 8oxG were much more severe than that for the template AP site, whereas with R357A the K_M values were similarly increased with all the three templates (Table 3). This suggested that R357 and L358 residues play distinct roles in DNA binding (see Discussion).

We found that one mutant, R357A exhibited a drastic change for dNTP discrimination on reactions with template G (Fig. 3),

Table 1
Kinetic analysis of REV1$^{(341-829)}$ for dCMP incorporation with various DNA templates. Kinetic assays were performed for 5 min in 25 μl reaction mixtures using 23 fmol REV1$^{(341-829)}$ and 2.5 pmol of the indicated primer-templates. The AP template contained a tetrahydrofuran as an AP site analog. To determine K_M values for dCTP, its concentrations ranged from 1 to 1000 μM. K_M and k_{cat} were evaluated from the plot of the initial velocity versus the dCTP concentration using a hyperbolic curve-fitting program. Data from two to four independent experiments were plotted together and the correlation coefficients (R^2) were more than 0.97.

Template	REV1[a]			REV1$^{(341-829)}$		
	k_{cat} (s^{-1})	K_M (μM)	k_{cat}/K_M ($s^{-1}M^{-1}$)	k_{cat} (s^{-1})	K_M (μM)	k_{cat}/K_M ($s^{-1}M^{-1}$)
G	0.050	0.54	93000	0.073	0.33	220000
A	0.052	23	2300	0.080	29	2800
T	0.027	180	150	0.062	100	610
C	0.030	170	180	0.058	100	560
AP	0.082	7.6	11000	0.13	11	12000

[a] Data from a Ref. [9].

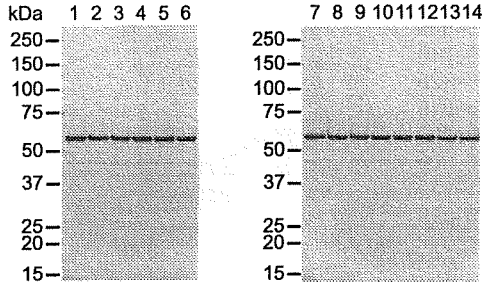

Fig. 2. Sodium dodecyl sulfate–polyacrylamide gel electrophoresis of purified REV1 mutants. The purified proteins (1 μg) were loaded on an 4–20% gradient polyacrylamide gel and stained with Coomassie Brilliant Blue R-250. lane 1, REV1$^{(341-829)}$; lane 2, F348A; lane 3, H359A; lane 4, S356A; lane 5, R357A; lane 6, L358A; lane 7, REV1$^{(341-829)}$; lane 8, R357A; lane 9, R357K; lane 10, R357S; lane 11, R357G; lane 12, R357T; lane 13, R357Q; lane 14, R357M.

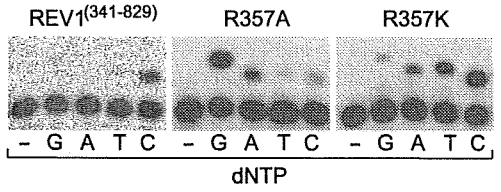

Fig. 3. Altered substrate specificity of R357A and R357K mutants. REV1$^{(341-829)}$ (23 fmol) R357A (26 fmol) or R357K (44 fmol) were incubated under standard reaction conditions with 100 nM of template G and 0.1 mM of each dNTP at 30 °C for 10 min. The reaction products were resolved in 20% polyacrylamide gels containing 8 M urea, and autoradiographed at −80 °C.

the K_M for dCTP being increased 240-fold (Table 4). Surprisingly, the K_M for dGTP, an inappropriate nucleotide, was decreased to 23 μM from 300 μM for the wild-type (Table 4). The efficiencies of dGMP incorporation opposite template G and template 8oxG of the mutant were similar to that for dCTP incorporation opposite template 8oxG of the wild-type (Table 4).

For further analysis of mechanisms of dNTP discrimination by R357, we replaced the arginine residue to lysine, serine, glycine, threonine, glutamine, and methionine. The mutant proteins were purified with equivalent qualities (Fig. 2). Regarding substrate specificity of these mutants under standard assay conditions we found that the properties of R357S, R357G, R357T, R357Q, and R357M were similar to that of R357A having preference for dGTP, while R357K was unique (Fig. 3, data not shown). Consequently, we selected R357K and R357S for further kinetic analysis. The kinetic parameters of the mutant R357S demonstrated similarity to those for R357A, exhibiting preference for dGTP (Table 4). In contrast, R357K retained the preference for dCTP and exhibited slightly higher activities for incorporation of dATP and dTTP on the template G (Table 4).

Table 2
Kinetic analysis of REV1$^{(341-829)}$ and mutants for dCMP incorporation with various DNA templates. Kinetic assays were performed for 5 min in 25 μl reaction mixtures using 2.5 pmol of the indicated primer-templates. The enzyme concentrations ranged from 44 fmol to 1.8 pmol. To determine K_M values for dCTP, its concentrations ranged from 1 to 1000 μM. K_M and k_{cat} were evaluated from the plot of the initial velocity versus the dCTP concentration using a hyperbolic curve-fitting program. Fold reduction of k_{cat} values is shown in parenthesis. Data from two to four independent experiments were plotted together and the correlation coefficients (R^2) were more than 0.97.

Protein	Template G			Template 8oxG			Template AP		
	k_{cat} (s^{-1})		K_M (μM)	k_{cat} (s^{-1})		K_M (μM)	k_{cat} (s^{-1})		K_M (μM)
REV1$^{(341-829)}$	0.073	(1.0)	0.33	0.032	(1.0)	9.1	0.13	(1.0)	11
F348A	0.065	(1.1)	0.79	0.027	(1.1)	3.1	0.053	(2.5)	32
S356A	0.068	(1.1)	10	0.033	(1.0)	7.7	0.014	(9.5)	78
R357A	0.025	(3.0)	79	0.017	(1.9)	57	0.0023	(57)	920
L358A	0.022	(3.4)	71	0.0042	(7.6)	29	0.0032	(42)	490
H359A	0.080	(1.0)	35	0.028	(1.1)	8.1	0.015	(9.2)	160

Table 3
Kinetic analysis of REV1$^{(341-829)}$ and mutants, R357A and L358A, for various DNA templates. Kinetic assays were performed for 5 min in 25 μl reaction mixtures using indicated templates with 88 fmol of REV1$^{(341-829)}$, 1.8 pmol of R357A and L358A. To determine K_M values for the templates, the concentrations ranged from 10 nM to 100 nM. The dCTP concentration was fixed at 100 μM. K_M and k_{cat} values were evaluated from the plot of the initial velocity versus the template concentrations using a hyperbolic curve-fitting program. Data from two to four independent experiments were plotted together and the correlation coefficients (R^2) were more than 0.94.

Protein	Template G K_M (nM)	Template 8oxG K_M (nM)	Template AP K_M (nM)
REV1$^{(341-829)}$	28	40	45
R357A	120	230	190
L358A	110	360	78

Table 4
Kinetic analysis of REV1$^{(341-829)}$ R357 mutants for dNMP incorporation with various DNA templates. Kinetic assays were performed for 5 min in 25 μl reaction solutions using 2.5 pmol of the indicated primer-templates. The enzyme concentrations ranged from 44 fmol to 88 fmol. To determine K_M values for dNTPs, the concentrations ranged from 1 to 1000 μM. K_M and k_{cat} were evaluated from the plot of the initial velocity versus the dCTP concentration using a hyperbolic curve-fitting program. Data from two to four independent experiments were plotted together and the correlation coefficients (R^2) were more than 0.95.

dNTP	Template G		Template 8oxG		Template AP	
	k_{cat} (s^{-1})	K_M (μM)	k_{cat} (s^{-1})	K_M (μM)	k_{cat} (s^{-1})	K_M (μM)
REV1$^{(341-829)}$						
G	0.097	300	0.014	72	0.0027	260
A	0.0037	420	0.00075	95	0.00035	680
T	0.048	200	0.014	79	0.0033	410
C	0.073	0.33	0.032	9.1	0.13	11
R357A						
G	0.097	23	0.043	27	0.014	190
A	0.080	48	0.028	56	0.0032	130
T	0.0058	100	0.0098	68	0.0020	580
C	0.025	79	0.017	57	0.0023	920
R357K						
G	0.014	340	0.0075	310	0.00042	380
A	0.027	210	0.012	88	0.0010	240
T	0.028	100	0.015	84	0.0015	270
C	0.042	31	0.045	82	0.0032	380
R357S						
G	0.088	25	0.037	9.2	0.014	170
A	0.047	130	0.023	44	0.0023	450
T	0.013	68	0.0078	35	0.0022	770
C	0.035	84	0.014	21	0.0025	960

Discussion

Although REV1 is a member of Y-family DNA polymerases and the amino acid sequence is well conserved among the members, its catalytic activity is restricted to utilization of dCTP as the dNTP source with a preference for a guanine residue as the template. Deletion analyses here revealed that an extra domain named the N-digit is essential for dCMP transferase activity of REV1, as reported previously [11,12]. This domain is conserved only in the REV1 family but not other Y-family polymerases, suggesting a crucial role for dCMP transferase activity. In this study, we determined for the first time the K_M values for templates. When each of R357 and L358 residues was replaced with alanine, the K_M values were increased. Interestingly, the defect of L358A was not as severe with template F as with the templates G and 8oxG, suggesting that the leucine residue might be crucial for binding to template G and damaged bases, but not the AP site. This is consistent with the model from the crystal structure and suggests that the leucine residue evicts template G from the DNA helix, then taking up much of the vacated space [12]. L358 could thus play a positive role in pushing out the base moiety. In this situation, R357 forms a hydrogen bond with the 5′ phosphate of the ejected template G [12]. Lack of this interaction on the R357A mutant could result in lowered affinity for template DNA.

When the R357 residue was replaced with others, the specificity for dCTP was altered. The kinetic analysis demonstrated that the arginine residue has a crucial function for selective utilization of dCTP. This result also is in good agreement with the model suggested by the crystal structure that the arginine residue forms hydrogen bonds with the cytidine residue of an incoming dCTP [12]. Besides, other amino acid residues surrounding the nucleotide binding pocket could also interact with the cytidine residue, since R357K mutant still retained a significant selectivity for dCTP. Furthermore, our analysis using mutants revealed that the nucleotide binding pocket has a significant but latent affinity for dGTP. When the R357 residue was replaced with other amino acids, in most of the cases, the enzyme lost affinity for dCTP, whereas an affinity for dGTP was obtained. Only in the case of the lysine was the affinity for dGTP rather reduced. It has been established that utilization of dGTP is an intrinsic property of wild-type REV1 [7–10,15]. The results suggest that surrounding amino acid residues in the nucleotide binding pocket except for the R357 residue probably have the potential to stabilize incoming dGTP. A positive charge of arginine or lysine could prevent such interaction with dGTP. Therefore, we suggest that R357 has two functions, which are specific interaction with dCTP and prevention of dGTP binding. We propose that both direct and indirect mechanisms ensure specificity for dCTP.

Our results also demonstrated significance of the SRLH motif for reaction with template AP sites. Mutations not only in R357 and L358 residues, but also S356 and H359, much reduced the transferase activity. Especially, the L358 residue could optimize the binding to a template AP site by occupying the empty space. A SRLH motif could be required for accurate arrangement of the template AP site and dCTP with the active site of REV1.

Many studies have demonstrated in yeast that the deoxycytidyl transferase activity of Rev1 is responsible for bypass synthesis of AP sites in different experimental systems, in which a gapped plasmid [16,17] or oligonucleotides containing an AP site [18–20] were transfected into yeast cells. Furthermore, expression of altered human uracil-DNA glycosylases that remove undamaged cytosines or thymines, was found to result in Rev1 dependent incorporation of dCMP opposite template AP site, generated by the glycosylases in yeast cells [21]. In spite of the elegant mechanisms of the enzyme to ensure incorporation of dCTP [11,12] and accumulating *in vivo* evidence, biological significance for insertion of dCMP is still obscure. In this study, we found novel mutants, which can incorporate dGMP with higher efficiency than dCMP. These could be useful for further analysis *in vivo* to address the biological significance for insertion of dCMP.

In conclusion, our experimental data suggest functional roles of conserved amino acid residues involved in substrate discrimination and template binding of the human REV1 protein. The proposed molecular mechanisms are supported by the model reported recently from crystallography. Furthermore, the mutants obtained in this study should facilitate further analysis *in vivo* to address the biological significance for insertion of dCMP by REV1.

Conflict of interest

None.

Acknowledgments

We are grateful to Kumiko Mizuno, Tomoka Nakashima, Masako Okii, Fumie Okubo, Kazumi Shimamoto, Hatsue Wakayama, and Mai Yoshida for their laboratory assistance. This work was supported by Grants-in-Aid from the Ministry of Education, Culture, Sports, Science and Technology of Japan (to Y.M. and K.K.), by the 21st Century Center of Excellence program from the Ministry of Education, Culture, Sports, Science and Technology of Japan (to K.K.), by Health and Labour Science Research Grants (to K.K.) and by Grants-in-Aid for Cancer Research from the Ministry of Health, Labour and Welfare (to K.K.). J.P. was supported by a JSPS Research Fellowship for Young Scientists.

References

[1] S.D. McCulloch, T.A. Kunkel, The fidelity of DNA synthesis by eukaryotic replicative and translesion synthesis polymerases, Cell Res. 18 (2008) 148–161.
[2] H. Ohmori, E.C. Friedberg, R.P. Fuchs, M.F. Goodman, F. Hanaoka, D. Hinkle, T.A. Kunkel, C.W. Lawrence, Z. Livneh, T. Nohmi, L. Prakash, S. Prakash, T. Todo, G.C.

Walker, Z. Wang, R. Woodgate, The Y-family of DNA polymerases, Mol. Cell 8 (2001) 7–8.
[3] C. Masutani, R. Kusumoto, S. Iwai, F. Hanaoka, Mechanisms of accurate translesion synthesis by human DNA polymerase η, EMBO J. 19 (2000) 3100–3109.
[4] S. Prakash, R.E. Johnson, L. Prakash, Eukaryotic translesion synthesis DNA polymerases: specificity of structure and function, Annu. Rev. Biochem. 74 (2005) 317–353.
[5] J.R. Nelson, C.W. Lawrence, D.C. Hinkle, Deoxycytidyl transferase activity of yeast REV1 protein, Nature 382 (1996) 729–731.
[6] C.W. Lawrence, Cellular roles of DNA polymerase ζ and Rev1 protein, DNA Repair 1 (2002) 425–435.
[7] Y. Zhang, X. Wu, O. Rechkoblit, N.E. Geacintov, J.S. Taylor, Z. Wang, Response of human REV1 to different DNA damage: preferential dCMP insertion opposite the lesion, Nucleic Acids Res. 30 (2002) 1630–1638.
[8] Y. Masuda, M. Takahashi, S. Fukuda, M. Sumii, K. Kamiya, Mechanisms of dCMP transferase reactions catalyzed by mouse Rev1 protein, J. Biol. Chem. 277 (2002) 3040–3046.
[9] Y. Masuda, K. Kamiya, Biochemical properties of the human REV1 protein, FEBS Lett. 520 (2002) 88–92.
[10] L. Haracska, S. Prakash, L. Prakash, Yeast Rev1 protein is a G template-specific DNA polymerase, J. Biol. Chem. 277 (2002) 15546–15551.
[11] D.T. Nair, R.E. Johnson, L. Prakash, S. Prakash, A.K. Aggarwal, Rev1 employs a novel mechanism of DNA synthesis using a protein template, Science 309 (2005) 2219–2222.
[12] M.K. Swan, R.E. Johnson, L. Prakash, S. Prakash, A.K. Aggarwal, Structure of the human Rev1–DNA–dNTP ternary complex, J. Mol. Biol. 390 (2009) 699–709.
[13] Y. Masuda, M. Takahashi, N. Tsunekuni, T. Minami, M. Sumii, K. Miyagawa, K. Kamiya, Deoxycytidyl transferase activity of the human REV1 protein is closely associated with the conserved polymerase domain, J. Biol. Chem. 276 (2001) 15051–15058.
[14] Y. Masuda, K. Kamiya, Role of single-stranded DNA in targeting REV1 to primer termini, J. Biol. Chem. 281 (2006) 24314–24321.
[15] C.A. Howell, S. Prakash, M.T. Washington, Pre-steady-state kinetic studies of protein-template-directed nucleotide incorporation by the yeast Rev1 protein, Biochemistry 46 (2007) 13451–13459.
[16] P.E. Gibbs, C.W. Lawrence, Novel mutagenic properties of abasic sites in *Saccharomyces cerevisiae*, J. Mol. Biol. 251 (1995) 229–236.
[17] J.R. Nelson, P.E. Gibbs, A.M. Nowicka, D.C. Hinkle, C.W. Lawrence, Evidence for a second function for *Saccharomyces cerevisiae* Rev1p, Mol. Microbiol. 37 (2000) 549–554.
[18] C. Otsuka, S. Sanadai, Y. Hata, H. Okuto, V.N. Noskov, D. Loakes, K. Negishi, Difference between deoxyribose- and tetrahydrofuran-type abasic sites in the *in vivo* mutagenic responses in yeast, Nucleic Acids Res. 30 (2002) 5129–5135.
[19] C. Otsuka, K. Kobayashi, N. Kawaguchi, N. Kunitomi, K. Moriyama, Y. Hata, S. Iwai, D. Loakes, V.N. Noskov, Y. Pavlov, K. Negishi, Use of yeast transformation by oligonucleotides to study DNA lesion bypass *in vivo*, Mutat. Res. 502 (2002) 53–60.
[20] C. Otsuka, N. Kunitomi, S. Iwai, D. Loakes, K. Negishi, Roles of the polymerase and BRCT domains of Rev1 protein in translesion DNA synthesis in yeast *in vivo*, Mutat. Res. 578 (2005) 79–87.
[21] P. Auerbach, R.A. Bennett, E.A. Bailey, H.E. Krokan, B. Demple, Mutagenic specificity of endogenously generated abasic sites in *Saccharomyces cerevisiae* chromosomal DNA, Proc. Natl. Acad. Sci. USA 102 (2005) 17711–17716.

Biochemical and Biophysical Research Communications 391 (2010) 542–546

Contents lists available at ScienceDirect

Biochemical and Biophysical Research Communications

journal homepage: www.elsevier.com/locate/ybbrc

Roles of POLD4, smallest subunit of DNA polymerase δ, in nuclear structures and genomic stability of human cells

Qin Miao Huang [a], Tomohiro Akashi [b], Yuji Masuda [c], Kenji Kamiya [c], Takashi Takahashi [a], Motoshi Suzuki [a,*]

[a] Division of Molecular Carcinogenesis, Center for Neurological Diseases and Cancer, Nagoya University Graduate School of Medicine, Nagoya, Japan
[b] Division of Molecular Mycology and Medicine, Center for Neurological Diseases and Cancer, Nagoya University Graduate School of Medicine, Nagoya, Japan
[c] Research Institute for Radiation Biology and Medicine, Hiroshima University, Hiroshima 734-8553, Japan

ARTICLE INFO

Article history:
Received 13 November 2009
Available online 24 November 2009

Keywords:
POLD4
Karyomere
Micronuclei
Cell cycle
DNA replication
DNA damage

ABSTRACT

Mammalian DNA polymerase δ (pol δ) is essential for DNA replication, though the functions of this smallest subunit of POLD4 have been elusive. We investigated pol δ activities *in vitro* and found that it was less active in the absence of POLD4, irrespective of the presence of the accessory protein PCNA. shRNA-mediated reduction of POLD4 resulted in a marked decrease in colony formation activity by Calu6, ACC-LC-319, and PC-10 cells. We also found that POLD4 reduction was associated with an increased population of karyomere-like cells, which may be an indication of DNA replication stress and/or DNA damage. The karyomere-like cells retained an ability to progress through the cell cycle, suggesting that POLD4 reduction induces modest genomic instability, while allowing cells to grow until DNA damage reaches an intolerant level. Our results indicate that POLD4 is required for the *in vitro* pol δ activity, and that it functions in cell proliferation and maintenance of genomic stability of human cells.

Introduction

Eukaryotic DNA polymerase δ (pol δ), a key enzyme that participates in DNA replication and repair, consists of four subunits; POLD1 (catalytic subunit, alternatively called p125), POLD2 (p50), POLD3 (p68), and POLD4 (p12) [1,2]. Among those, POLD4 binds to POLD1, POLD2, and an accessory protein of PCNA, which allows pol δ to exhibit its full activity [1,3].

A previous study showed that the *POLD4* ortholog of *Cdm1* in *Schizosaccharomyces pombe* is a non-essential gene related to cell growth, division, and sensitivity to DNA damaging reagents [4]. *Saccharomyces cerevisiae* does not have a POLD4 counterpart, indicating that POLD4 is dispensable in lower eukaryotic cells. In contrast, siRNA-mediated knockdown of POLD4 caused a significant decrease in the proliferation rate of FGF2-activated mouse-endothelial cells [5]. However, it remains unknown whether POLD4 is required for other types of mammalian cells, such as those related to human cancer, or if it has additional functions in mammalian cells.

In the present study, we analyzed the roles of POLD4 for cell proliferation in human lung cancer cell lines. Our findings indicate that POLD4 is required for maintaining the proper nuclear structures and suggest that the pathological structures reflect elevated DNA damage in chromosomes.

* Corresponding author. Address: Division of Molecular Carcinogenesis, Center for Neurological Diseases and Cancer, Nagoya University Graduate School of Medicine, Nagoya 466-8550, Japan.
E-mail address: msuzuki@med.nagoya-u.ac.jp (M. Suzuki).

0006-291X/$ - see front matter © 2009 Elsevier Inc. All rights reserved.
doi:10.1016/j.bbrc.2009.11.094

Materials and methods

Antibodies. The antibodies used in this study were anti-POLD4 (POLD4 subunit of pol δ) ascites (2B11, Abnova, Taipei City, Taiwan), anti-lamin B (c-20) (Santa Cruz Biotechnology, Santa Cruz, CA), and anti-γ-tubulin (Sigma–Aldrich, St. Louis, MO).

In vitro pol δ activity. Three- and 4-subunit DNA from pol δ were expressed in *Escherichia coli*, and purified as described previously [6]. pol δ activity was determined in a reaction mixture (25 μl) containing 20 mM HEPES–NaOH (pH 7.5), 50 mM NaCl, 0.2 mg/ml BSA, 1 mM dithiothreitol, 10 mM $MgCl_2$, 1 mM ATP, 0.1 mM each of dGTP, dATP, dCTP, and [α-^{32}P]dTTP, 100 ng poly dA-oligo dT (GE Healthcare, Piscataway, NJ), 86 ng (1.0 pmol as a trimer) of PCNA, and 11–88 ng (46–372 fmol) of pol δ at 30 °C for 10 min. Following incubation, the reactions were terminated with 2 μl of 300 mM EDTA. pol activity was determined with reference to the incorporation of [α-^{32}P]dTMP, as previously described [6].

Colony formation assay. To assess cell proliferation, colony formation assays were performed as previously described [7]. In order to rule out the off-target effect, we designed two independent DNA sequences as follows: MS543F, 5′-GATCCCCagtctctggcatctctatcATTCAAGAGATgatagagatgccagagactTTTTTGGAAA-3; MS544R, 5′-AGCTTTTCCAAAAAagtctctggcatctctatcATCTCTTGAATgatagagatgccagagactGGG-3; MS551F, 5′-GATCCCCgcatctctatcccctatgaATTCAAGAGATtcataggggatagagatgcTTTTTGGAAA-3; and MS552R, 5′-AGCTTTTCCAAAAAgcatctctatccccctatgaATCTCTTGAATtcataggggatagagatgcGGG-3, in which the targeting sequences are indicated in lowercase letters. To construct shRNA vectors, MS543F and MS544R

(polD4-5), and MS551F and MS552R (polD4-3-1) were annealed, then inserted between the restriction sites BglII and HindIII in PH1RNAneo [7]. Cells transfected with a vector carrying either polD4-3-1 or polD4-5 were cultured in media containing 1 mg/ml G418 (Invitrogen, Carlsbad, CA 10131-027), which was reduced by 0.2 mg/ml every 2 days until it reached 0.4 mg/ml. When colonies grew to visible seizes, they were fixed by cold methanol for 5 min and stained with 4% Giemsa for 15 min at room temperature.

RNA interference. Transfection was carried out using 50 nmol/L of a small interfering RNA (siRNA) duplex (Sigma–Aldrich) targeting each mRNA, or negative control 1# (Ambion) with Lipofectamine-2000 (Invitrogen). The sequences of si*POLD4* were the same as those of polD4-3-1: *POLD4* (si*D4*) sense, 5′-GCAUCUCUAUCCCCUAUGATT-3′; and antisense, 5′-UCAUAGGGGAUAGAGAUGCTT.

Laser scanning cytometry (LSC). Following an overnight culture, 3×10^5/ml Calu6 cells on coverslips were fixed by cold methanol, washed with PBS, and incubated with 1 mg/ml RNase A in 50 mM Tris–HCl, pH 7.5, at 37 °C for 1 h. Cells were further treated with 50 μg/ml propidium iodide in a mixture containing 180 mM Tris–HCl, pH 7.5, 180 mM NaCl, and 70 mM $MgCl_2$ for 15 min. Nuclei structures and DNA contents were analyzed using a Laser Scanning Cytometer (LSC, Olympus, Tokyo, Japan), with DNA content at the G1 peak regarded as 2N, though Calu6 cells carry a greater amount of DNA chromatin than normal cells.

Cell cycle synchronization. Calu6 cells were synchronized according to the method of Nakagawa et al. [8], with minor modifications. In brief, 24-h treatment with 2 mM thymidine was used to arrest exponentially proliferating cells in the S phase. Cells were then released from arrest by three washes in PBS and grown in fresh medium for 15 h, then 1 μM of aphidicolin was used for the second block for 10 h. After releasing by three washes in PBS, cells were incubated in RPMI1640 containing 5% fetal bovine serum and harvested at various time points.

Immunofluorescence. Following an overnight culture, 3×10^5/ml Calu6 cells on coverslips were transfected with siRNA as described above. After 48 h, they were fixed in 4% paraformaldehyde for 10 min at room temperature, followed by treatment with cold methanol for 2 min. The coverslips were washed three times in PBS, treated with PBS containing 0.25% Triton X-100 on ice for 30 min, and incubated with anti-lamin B or anti-γ-tubulin antibody overnight at 4 °C. The cells were then washed three times in PBS, incubated for 1 h with Alexa 488-conjugated secondary antibody (Molecular Probes, OR, USA), and analyzed using an Olympus BX60 (Olympus).

Results and discussion

DNA synthesis activities of pol δ with or without POLD4 in vitro

In order to analyze POLD4 functions related to intrinsic pol δ activity, 3- and 4-subunit structures of pol δ were expressed and purified. In the absence of POLD4, pol δ was less active than the holoenzyme in a reaction containing poly dA–dT as a template primer (Fig. 1A), with a similar result obtained when the accessory protein of PCNA was omitted from the reaction (Fig. 1B). These results are consistent with those of previous studies [1,3] and indicate that POLD4 is required for pol δ to exhibit its full catalytic activity.

POLD4 required for cell proliferation

A previous genetic study of *S. pombe* demonstrated that the *POLD4* ortholog of *Cdm1* is a non-essential gene for cell growth,

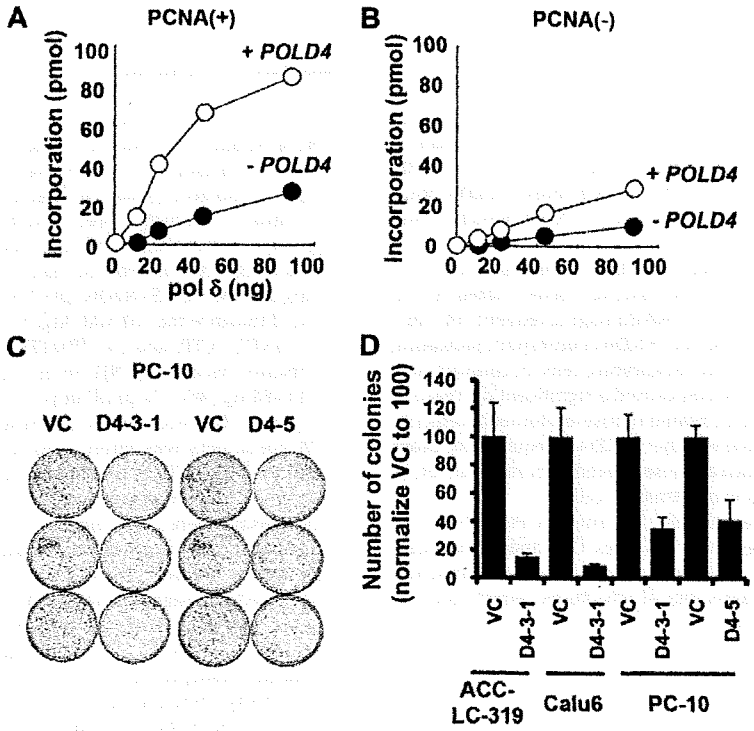

Fig. 1. *In vitro* DNA synthesis activities of pol δ and effect of POLD4 depletion on colony formation activity. (A) pol δ activities were measured and plotted as described in Materials and methods. (B) The same reactions were carried out in the absence of PCNA. (C) PC-10 was used for transfection with plasmids carrying either D4-3-1 or D4-5, and colony formation activity was determined as described in Materials and methods. VC represents vector control. (D) Results of the colony formation assay were plotted in a graph.

division, and sensitivity to DNA damaging reagents [4]. Nevertheless, it is possible that mammalian cells with larger genomic sizes require POLD4 for efficient and accurate DNA replication. We investigated this possibility using shRNA-mediated knockdown of *POLD4*. As shown in Fig. 1C, two independent sequences of shRNA caused reduced activity in a colony formation assay using PC-10, a human non-small cell lung cancer (NSCLC) cell line. Similar results were obtained with different NSCLC cell lines, Calu6 and ACC-LC-319 (Fig. 1D). These findings suggest that human cells require POLD4 for proliferation.

Structure and population of karyomere-like cells following siPOLD4 treatment

Since pol δ is a major DNA replication and repair polymerase, impairment of its activity may cause DNA replication stress, such as accumulation of single-stranded DNA gaps, and inefficient repair of endogenous DNA damage, which ultimately results in cell death. On the other hand, it is also possible that some cells continue to grow following such genetic erosion, which may cause genomic instability. Therefore, we investigated whether POLD4 is also required for suppressing genomic instability in human cells. Initially, we attempted to establish stable clones with low POLD4 expression using shRNA-treated cells. However, clones with adequate levels of POLD4 expression were gradually selected, leading to recovery to the original level over time (data not shown). Therefore, in the following experiments, we used siRNA to transiently reduce POLD4 expression (Fig. 2A, left).

Calu6 cells treated with si*POLD4* formed multiple or lobed nuclei, at a 5.3-fold greater frequency than in the control experiment (Fig. 2B and C). Similar structures were also observed when A549 cells were treated with si*POLD4* (data not shown). Staining with

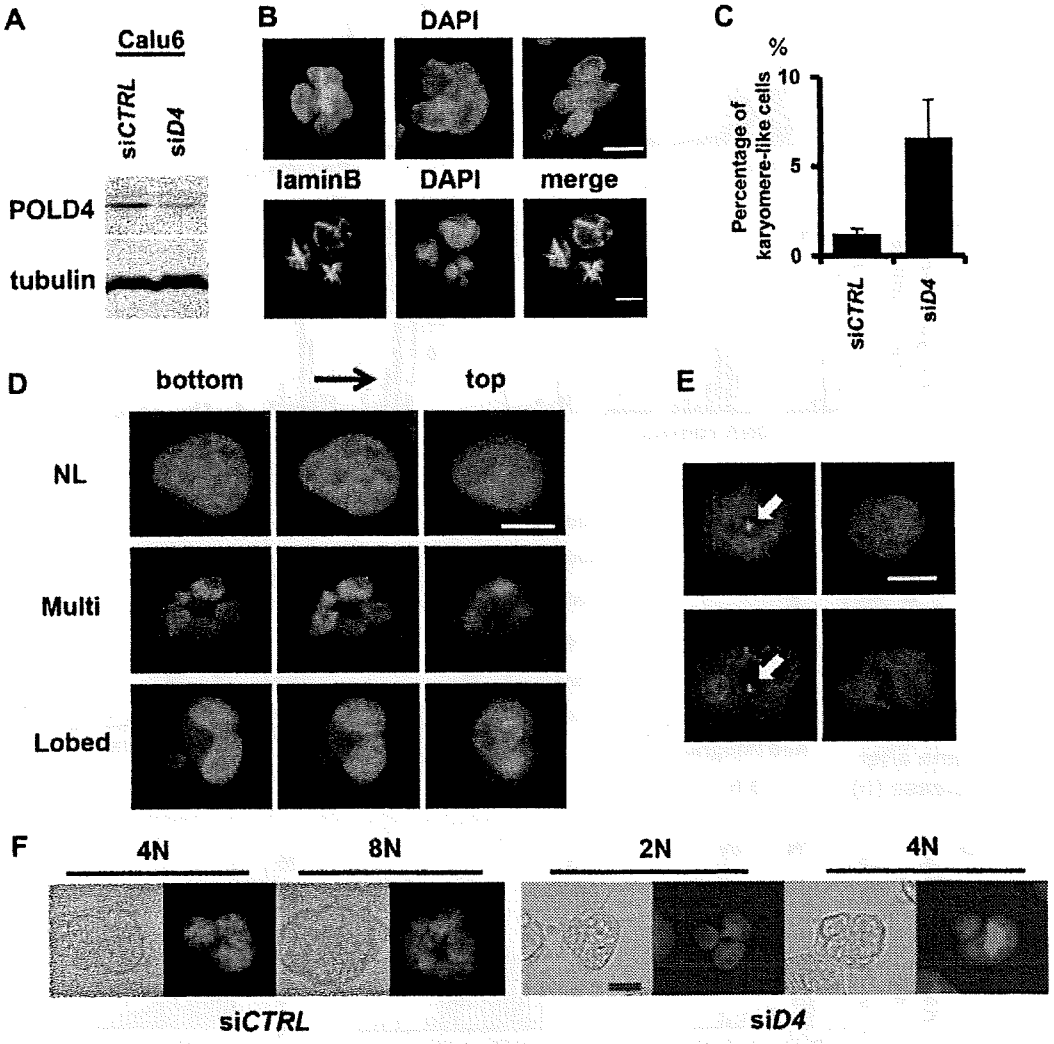

Fig. 2. Structures and population of karyomere-like cells upon si*POLD4* treatment. (A) Western blot analysis of POLD4 and α-tubulin in protein extracts from si*POLD4*- or si*CTRL*-treated Calu6 cells. (B) Upper panels: Calu6 cells were treated with si*POLD4* for 48 h and stained with DAPI. Sample karyomere-like nuclei are shown. Lower panels: Calu6 cells were treated with si*POLD4* for 48 h, then visualized with anti-lamin B antibody or DAPI. (C) Calu6 cells were treated with si*POLD4* or si*CTRL*, then the frequencies of karyomere-like structures in 1000 cells were counted and plotted. In this experiment, cells with three or more nuclear lobes, or three or more nuclei were regarded as karyomere-like cells. Averages of three independent results are shown with SD. (D) si*POLD4*-treated cells were stained by DAPI, then three sequential photographs were taken every 4 μm from the bottom. Upper, middle, and lower panels show images of normal, multiple, and lobed nuclear structures, respectively. (E) After being treated with si*POLD4*, cells were visualized with anti-γ-tubulin (left) or DAPI (right). Upper and lower panels show representative pictures of normal and karyomere-like nuclei, respectively. Centrosomes are indicated by arrows. (F) LSC analysis. Phase-contrast and propidium iodide-stained images of karyomere-like cells among 4N and 8N (si*CTRL*), or 2N and 4N (si*POLD4*) cells. Bar indicates 10 μm.

the anti-lamin B antibody outlined the edges of the DAPI structures and showed that the nuclear envelope was formed around chromatin (Fig. 2B, lower). Sequential acquisition of images from the bottom of the cells further illustrated the abnormal structures of single cells, including a flat profile and multiple nuclei (Fig. 2D, middle panels), or a single nucleus associated with multiple lobes (Fig. 2D, lower panels). For both types of abnormal structures, the nuclear sizes were approximately that of a normally shaped nucleus (Fig. 2D, upper panels).

The multiple nuclei seen with these structures were reminiscent of 'micronuclei' that indicated the presence of DNA damage and DNA replication stress in previous studies [9–11], while the lobed nuclei closely resembled 'karyomere' nuclei observed in zebrafish blastomeres [12] and early *Xenopus laevis* development [13]. In that latter study and other studies referenced therein, it was suggested that karyomere formation is a physiological mitotic process that may share similar mechanisms with pathological micronuclei formation; with both multiple and lobed nuclei, isolated chromosomes might

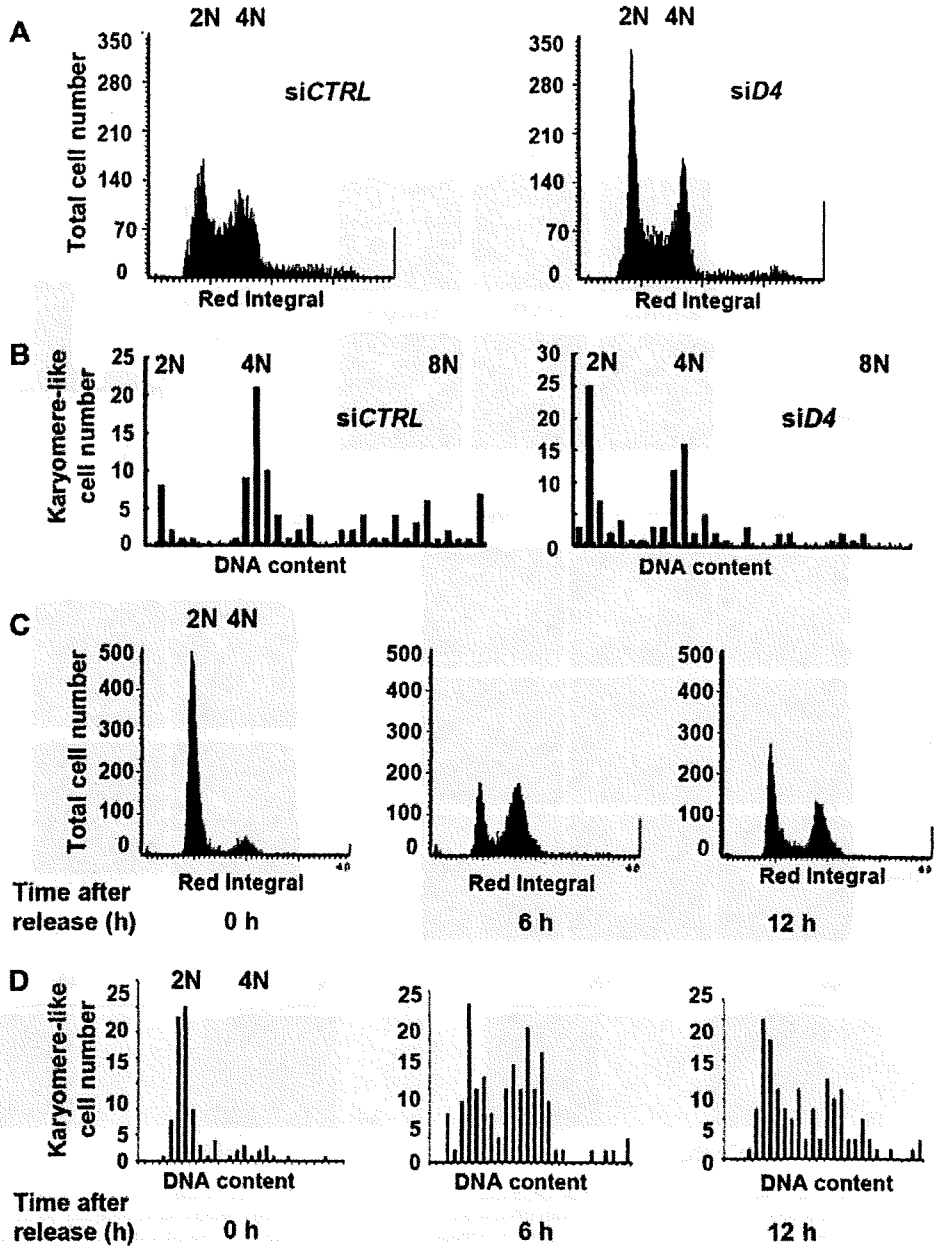

Fig. 3. Cell cycle dynamics of karyomere-like cells. (A) Calu6 cells were treated with si*CTRL* (left) or si*POLD4* (right), then their DNA contents were subjected to LSC analysis. The G1 population found among the majority of cells was regarded as 2N. (B) In the same experiment, DNA contents of 100 karyomere-like cells were determined. Cell numbers in each DNA content range were plotted with histograms. (C) Calu6 cells were treated with si*POLD4*, then synchronized at the G1/S boundary and released for cell cycle progression. At 0, 6, or 12 h after release, DNA contents were subjected to LSC. (D) In the same experiment, the DNA contents of 100 karyomere-like cells were measured. Cell numbers in each DNA content range were plotted with histograms.

be surrounded by a nuclear envelope after chromosome segregation occurs. Therefore, those two types of abnormal structures are referred to as karyomere-like nuclei hereafter.

In addition to DNA damage, formation of karyomere-like nuclei may also occur as a consequence of dysfunctions of the mitotic apparatus [13,14]. Moreover, a previous study found that the anti-POLD4 antibody bound the surface of mitotic chromosomes, which suggests specific functions of POLD4 during mitosis [5]. To investigate this, we analyzed the centrosome structures in si *POLD4*-treated cells, as it has been reported that disturbed chromosomal migration occurred with abnormal replication or localization of centrosomes [15,16]. Our present results showed that si *POLD4*-treated cells were associated with normal centrosome structures, which had one or two centrosomes located at a single site (Fig. 2E). We also quantified the lagging-chromosome frequencies, and found that they were very similar between si*POLD4*- and si*CTRL*-treated mitotic cells (data not shown). Although the results of this limited experiment were contrary to our speculation that POLD4 has some mitotic functions, we intend to conduct more detailed examinations in the future.

Cell cycle dynamics of karyomere-like cells

In the following experiments, we studied the cell cycle dynamics of karyomere-like cells. After si*POLD4* treatment, we observed checkpoint activation (data not shown, detailed mechanisms discussed elsewhere), and accumulations of G1- and G2-populations (Fig. 3A). In si*CTRL*-treated cells, most of the karyomere-like populations were found among the minor aneuploid populations (Figs. 3B and 2F, left panels). In contrast, karyomere-like cells in si *POLD4*-treated cells were found to have normal ploidy as seen with 2N–4N cells (Fig. 3B, 2F, right panels).

In order to determine if karyomere-like cells remained alive and had an ability to progress through the cell cycle, we synchronized cells at the G1–S boundary, then released them and observed the cell cycle progression, as well as the associated nuclear shapes (Fig. 3C–E). Interestingly, karyomere-like cells progressed through the cell cycle and returned to G1 at 12 h after release. In support of these results, most karyomere-like cells were negative in TUNEL staining findings (data not shown). Therefore, these structures may not reflect the pro-apoptotic phenotype. Our results suggest that most karyomere-like cells are able to proliferate until they became arrested at the G1 or G2 phase, when DNA damage reaches an intolerant level.

In conclusion, our results showed that POLD4 supports cellular proliferation and suppresses karyomere-like nuclei formation in human cells, which might occur as a consequence of impairment of the DNA replication and repair activities of pol δ. A future study to identify the direct link between POLD4 and mitotic functions may reveal the underlying mechanisms to maintain genomic stability in human cells.

Acknowledgments

We thank Keiko Ueda and Makiko Terada for their initial involvement in this project. We are also grateful for Dr. Takeshi Senga of our university for the critical reading of the manuscript. This work was supported in part by a Grant-in-Aid for Scientific Research on Innovative Areas, a Grant-in-Aid for Scientific Research on Priority Areas from the Ministry of Education, Culture, Sports, Science, and Technology of Japan, and a Grant-in-Aid for Scientific Research from the Japan Society for the Promotion of Science.

References

[1] V.N. Podust, L.S. Chang, R. Ott, G.L. Dianov, E. Fanning, Reconstitution of human DNA polymerase delta using recombinant baculoviruses: the p12 subunit potentiates DNA polymerizing activity of the four-subunit enzyme, J. Biol. Chem. 277 (2002) 3894–3901.
[2] L. Liu, J. Mo, E.M. Rodriguez-Belmonte, M.Y. Lee, Identification of a fourth subunit of mammalian DNA polymerase delta, J. Biol. Chem. 275 (2000) 18739–18744.
[3] H. Li, B. Xie, Y. Zhou, A. Rahmeh, S. Trusa, S. Zhang, Y. Gao, E.Y. Lee, M.Y. Lee, Functional roles of p12, the fourth subunit of human DNA polymerase delta, J. Biol. Chem. 281 (2006) 14748–14755.
[4] N. Reynolds, A. Watt, P.A. Fantes, S.A. MacNeill, Cdm1, the smallest subunit of DNA polymerase d in the fission yeast *Schizosaccharomyces pombe*, is non-essential for growth and division, Curr. Genet. 34 (1998) 250–258.
[5] P. Dell'Era, S. Nicoli, G. Peri, M. Nieddu, M.G. Ennas, M. Presta, FGF2-induced upregulation of DNA polymerase-delta p12 subunit in endothelial cells, Oncogene 24 (2005) 1117–1121.
[6] Y. Masuda, M. Suzuki, J. Piao, Y. Gu, T. Tsurimoto, K. Kamiya, Dynamics of human replication factors in the elongation phase of DNA replication, Nucleic Acids Res. 35 (2007) 6904–6916.
[7] H. Tanaka, K. Yanagisawa, K. Shinjo, A. Taguchi, K. Maeno, S. Tomida, Y. Shimada, H. Osada, T. Kosaka, H. Matsubara, T. Mitsudomi, Y. Sekido, M. Tanimoto, Y. Yatabe, T. Takahashi, Lineage-specific dependency of lung adenocarcinomas on the lung development regulator TTF-1, Cancer Res. 67 (2007) 6007–6011.
[8] T. Nakagawa, Y. Hayashita, K. Maeno, A. Masuda, N. Sugito, H. Osada, K. Yanagisawa, H. Ebi, K. Shimokata, T. Takahashi, Identification of decatenation G2 checkpoint impairment independently of DNA damage G2 checkpoint in human lung cancer cell lines, Cancer Res. 64 (2004) 4826–4832.
[9] N. Holland, C. Bolognesi, M. Kirsch-Volders, S. Bonassi, E. Zeiger, S. Knasmueller, M. Fenech, The micronucleus assay in human buccal cells as a tool for biomonitoring DNA damage: the HUMN project perspective on current status and knowledge gaps, Mutat. Res. 659 (2008) 93–108.
[10] J.B. Bae, S.S. Mukhopadhyay, L. Liu, N. Zhang, J. Tan, S. Akhter, X. Liu, X. Shen, L. Li, R.J. Legerski, Snm1B/Apollo mediates replication fork collapse and S phase checkpoint activation in response to DNA interstrand cross-links, Oncogene 27 (2008) 5045–5056.
[11] D.J. Kirkland, L. Henderson, D. Marzin, L. Muller, J.M. Parry, G. Speit, D.J. Tweats, G.M. Williams, Testing strategies in mutagenicity and genetic toxicology: an appraisal of the guidelines of the European Scientific Committee for Cosmetics and Non-Food Products for the evaluation of hair dyes, Mutat. Res. 588 (2005) 88–105.
[12] V.K. Schoft, A.J. Beauvais, C. Lang, A. Gajewski, K. Prufert, C. Winkler, M.A. Akimenko, M. Paulin-Levasseur, G. Krohne, The lamina-associated polypeptide 2 (LAP2) isoforms beta, gamma and omega of zebrafish: developmental expression and behavior during the cell cycle, J. Cell Sci. 116 (2003) 2505–2517.
[13] J.M. Lemaitre, G. Geraud, M. Mechali, Dynamics of the genome during early *Xenopus laevis* development: karyomeres as independent units of replication, J. Cell Biol. 142 (1998) 1159–1166.
[14] M. Ohsugi, K. Adachi, R. Horai, S. Kakuta, K. Sudo, H. Kotaki, N. Tokai-Nishizumi, H. Sagara, Y. Iwakura, T. Yamamoto, Kid-mediated chromosome compaction ensures proper nuclear envelope formation, Cell 132 (2008) 771–782.
[15] D. Eriksson, P.O. Lofroth, L. Johansson, K.A. Riklund, T. Stigbrand, Cell cycle disturbances and mitotic catastrophes in HeLa Hep2 cells following 2.5 to 10 Gy of ionizing radiation, Clin. Cancer Res. 13 (2007) 5501s–5508s.
[16] H. Dodson, E. Bourke, L.J. Jeffers, P. Vagnarelli, E. Sonoda, S. Takeda, W.C. Earnshaw, A. Merdes, C. Morrison, Centrosome amplification induced by DNA damage occurs during a prolonged G2 phase and involves ATM, EMBO J. 23 (2004) 3864–3873.

THE JOURNAL OF BIOLOGICAL CHEMISTRY VOL. 284, NO. 38, pp. 25585–25592, September 18, 2009

Translesional DNA Synthesis through a C8-Guanyl Adduct of 2-Amino-1-methyl-6-phenylimidazo[4,5-*b*]pyridine (PhIP) *in Vitro*

REV1 INSERTS dC OPPOSITE THE LESION, AND DNA POLYMERASE κ POTENTIALLY CATALYZES EXTENSION REACTION FROM THE 3′-dC TERMINUS[*S]

Received for publication, June 25, 2009, and in revised form, July 16, 2009 Published, JBC Papers in Press, July 23, 2009, DOI 10.1074/jbc.M109.037259

Hirokazu Fukuda[‡], Takeji Takamura-Enya[§], Yuji Masuda[¶], Takehiko Nohmi[‖], Chiho Seki[‡], Kenji Kamiya[¶], Takashi Sugimura[‡], Chikahide Masutani[**], Fumio Hanaoka[1], and Hitoshi Nakagama[‡2]**

From the [‡]Biochemistry Division, National Cancer Center Research Institute, 1-1, Tsukiji 5, Chuo-ku, Tokyo 104-0045, the [§]Department of Applied Chemistry, Faculty of Engineering, Kanagawa Institute of Technology, Ogino 1030, Atsugi, Kanagawa 243-0292, the [¶]Department of Experimental Oncology, Research Institute for Radiation Biology and Medicine, Hiroshima University, Kasumi 1-2-3, Minami-ku, Hiroshima, Hiroshima 734-8553, the [‖]Division of Genetics and Mutagenesis, National Institute of Health Sciences, Kamiyoga 1-18-1, Setagaya-ku, Tokyo 158-8501, and the [**]Cellular Biology Laboratory, Graduate School of Frontier Biosciences, Osaka University, Yamada-oka 1-3, Suita, Osaka 565-0871, Japan

2-Amino-1-methyl-6-phenylimidazo[4,5-*b*]pyridine (PhIP) is the most abundant heterocyclic amine in cooked foods, and is both mutagenic and carcinogenic. It has been suspected that the carcinogenicity of PhIP is derived from its ability to form DNA adducts, principally dG-C8-PhIP. To shed further light on the molecular mechanisms underlying the induction of mutations by PhIP, *in vitro* DNA synthesis analyses were carried out using a dG-C8-PhIP-modified oligonucleotide template. In this template, the dG-C8-PhIP adduct was introduced into the second G of the TCC GGG AAC sequence located in the 5′ region. This represents one of the mutation hot spots in the rat *Apc* gene that is targeted by PhIP. Guanine deletions at this site in the *Apc* gene have been found to be preferentially induced by PhIP in rat colon tumors. DNA synthesis with A- or B-family DNA polymerases, such as *Escherichia coli* polymerase (pol) I and human pol δ, was completely blocked at the adducted guanine base. Translesional synthesis polymerases of the Y-family, pol η, pol ι, pol κ, and REV1, were also used for *in vitro* DNA synthesis analyses with the same templates. REV1, pol η, and pol κ were able to insert dCTP opposite dG-C8-PhIP, although the efficiencies for pol η and pol κ were low. pol κ was also able to catalyze the extension reaction from the dC opposite dG-C8-PhIP, during which it often skipped over one dG of the triple dG sequence on the template. This slippage probably leads to the single dG base deletion in colon tumors.

Heterocyclic amines (HCAs)[3] are naturally occurring genotoxic carcinogens produced from cooking meat (1). The initial carcinogenic event induced by HCAs is metabolic activation and subsequent covalent bond formation with DNA (1, 2). 2-Amino-1-methyl-6-phenylimidazo[4,5-*b*]pyridine (PhIP) is the most abundant heterocyclic amine in cooked foods, and was isolated from fried ground beef (3, 4). PhIP possesses both mutagenic and carcinogenic properties (5–8). Epidemiological studies have revealed that a positive correlation exists between PhIP exposure and mammary cancer incidence (9). PhIP induces colon and prostate cancers in male rats and breast cancer in female rats (8, 10).

The incidences of colon, prostate, and breast cancers are steadily increasing in Japan and other countries and this has been found to correlate with a more Westernized lifestyle. Elucidating the molecular mechanisms underlying PhIP-induced mutations is therefore of considerable interest. It is suspected that the carcinogenicity of PhIP is derived from the formation of DNA adducts, principally dG-C8-PhIP (11–14) (see Fig. 1). Studies of the mutation spectrum of PhIP in mammalian cultured cells and transgenic animals have revealed that G to T transversions are predominant and that guanine deletions from G stretches, especially from the 5′-GGGA-3′ sequence, are significant (15–20). Five mutations in the *Apc* gene were detected in four of eight PhIP-induced rat colon tumors, and all of these mutations involved a single base deletion of guanine from 5′-GGGA-3′ (21). These mutation spectra are thought to be influenced by various factors, including the primary structure of the target gene itself, the capacity of translesional DNA polymerases, and the activity level of repair enzymes (1). However, the molecular mechanisms underlying the formation of PhIP-induced mutations are largely unknown.

To shed further light on the molecular processes that underpin the mutations induced by PhIP, we performed *in vitro* DNA synthesis analyses using a dG-C8-PhIP-modified oligonucleotide template. We have recently reported the successful synthesis of oligonucleotides harboring a site-specific PhIP adduct

* This work was supported by Kakenhi Grant 19570144.
[S] The on-line version of this article (available at http://www.jbc.org) contains supplemental Table S1 and Figs. S1–S6.
[1] Present address: Dept. of Life Science, Faculty of Science, Gakushuin University, Mejiro 1-5-1, Toshima-ku, Tokyo 171-8588, Japan.
[2] To whom correspondence should be addressed. Tel.: 81-3-3542-2511; Fax: 81-33542-2530; E-mail: hnakagam@ncc.go.jp.
[3] The abbreviations used are: HCA, heterocyclic amines; PhIP, 2-amino-1-methyl-6-phenylimidazo[4,5-*b*]pyridine; TLS, translesional DNA synthesis; IQ, 2-amino-3-methylimidazo[4,5-*f*]quinoline; pol, DNA polymerase; DTT, dithiothreitol; PCNA, proliferating cell nuclear antigen; PIPES, 1,4-piperazinediethanesulfonic acid.

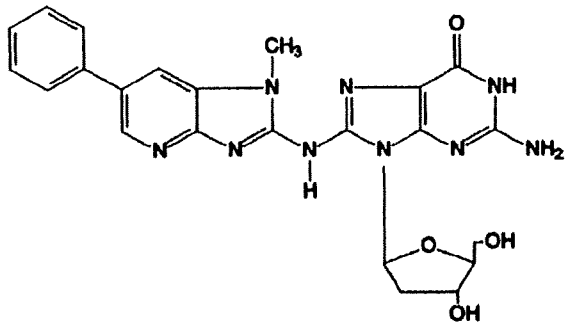

dG-C8-PhIP

FIGURE 1. **Structure of the dG-C8-PhIP adduct.**

(22). In our current study, we used this synthesis method to construct a 32-mer oligonucleotide template containing a 5′-TTCGGGAAC-3′ sequence with different site-specific PhIP adducts. We then utilized the resulting constructs in DNA synthesis analyses to reconstitute the PhIP-induced mutagenesis of the rat *APC* gene. DNA synthesis reactions with A- or B-family DNA polymerases, such as *Escherichia coli* pol I and human pol δ, or translesional synthesis (TLS) polymerases of the Y-family, pol η, pol ι, pol κ, and REV1, were carried out. Kinetic analyses of pol κ and REV1, for which TLS activities at the PhIP adduct were detected, were also performed.

EXPERIMENTAL PROCEDURES

Enzymes and Materials—T4 polynucleotide kinase and T4 DNA ligase were purchased from Toyobo Biochem (Osaka, Japan) and Takara Biotech (Tokyo Japan), respectively. Other materials were obtained from Sigma or Wako (Osaka, Japan).

DNA Polymerases and PCNA—Human recombinant DNA polymerases, pol δ, pol η, pol κ, and REV1, and PCNA were expressed and purified as described previously (23–27). Human DNA polymerase α and DNA polymerase ι were purchased from Chimerx. *E. coli* DNA polymerases I (Takara Biotech) and Klenow Fragment (Takara Biotech), and thermophilic bacterial DNA polymerases, r*Taq* (Toyobo Biochem) and *Tth* (Toyobo Biochem) were used.

Oligonucleotides—The method used to chemically synthesize three 9-mer oligonucleotides, 5′-TCCGGGAAC-3′, containing a PhIP adduct on either the first, second, or third G (p9B, p9C, and p9D, respectively) has been described previously (22). All other synthetic oligonucleotides were synthesized and purified using a reverse-phase cartridge (Operon Biotech Japan (Tokyo, Japan). The 23-mer oligonucleotides: p23a, 5′-TGACTCGTCGTGACTGGGAAAAC-3′, and p23b, 5′-GTCACGACGAGTCAGTTCCCGGA-3′, were used for constructing the template oligonucleotides as described below. A 32-mer oligonucleotide without the PhIP adduct, p32A, was used as a control template (see Table 1). Its 3′ complementary 29-, 28-, 27-, 26-, 22-, and 17-mer sequences (p29, p28, p27, p26, p22, and p17) were used as extension primers (see Table 1).

Construction of Template-Primer Complexes Containing the PhIP Adduct—A 32-mer template oligonucleotide p32C (see Table 1) was constructed by ligation of p9C with p23a as follows. The 5′-end of p23a was phosphorylated by T4 polynucleotide kinase and ATP. A mixture of p9C, p23a, and p23b (3 nmol each) in 250 μl of a buffer containing 5 mM Tris-HCl, 0.5 mM EDTA, 50 mM NaCl, pH 8.0, was denatured for 5 min at 95 °C, incubated for 10 min at 60 °C, and then cooled slowly to form the partial duplex structure of these three oligonucleotides (supplemental Fig. S1). The sample of the duplex oligonucleotide was mixed with 190 μl of Milli-Q water and 50 μl of ×10 ligation buffer (500 mM Tris-HCl (pH 7.5), 100 mM $MgCl_2$, 100 mM DTT, 10 mM ATP). Ligation was initiated by adding 10 μl of T4 DNA ligase (4,000 units), and the mixture was then incubated for 20 h at 16 °C. An additional incubation at 37 °C for 60 min was carried out after the addition of 1 μl of T4 DNA ligase, and the reaction was stopped by further incubation at 68 °C for 10 min. The p32C was separated by 18% PAGE containing 8 M urea, and excised and eluted as described previously (28). p32B and p32D were constructed using a similar method as for p9B and p9D, respectively (see Table 1). The purities of these oligonucleotides, p32B, p32C, and p32D, were determined by denatured PAGE after 5′-end labeling and UV absorbance at 260 and 370 nm.

Primer oligonucleotides were labeled with ^{32}P at the 5′-end as described previously (29), and then purified by MicroSpin™ G-25 or G-50 columns (GE Healthcare) as recommended by the supplier. The mixture of template and labeled primer (50 pmol each) in 400 μl of a buffer containing 8 mM Tris-HCl, 0.8 mM EDTA, 150 mM KCl (pH 8.0) was heated at 70 °C for 7 min, and then cooled slowly to room temperature. In the case of the substrates for TLS polymerases, pol η, pol ι, pol κ, and REV1, the final concentrations of template-primer and the constituents of the annealing buffers were changed to 500 nM and 10 mM Tris-HCl, 1 mM EDTA, and 50 mM NaCl (pH 8.0), respectively.

In Vitro DNA Synthesis Assay—A primer extension reaction was performed as described previously (30) with some modifications. Briefly, an aliquot of 0.75 μl of this primer-annealed template (final concentration, 12.5 nM) was mixed with 0.75 μl of ×10 Klenow buffer (100 mM Tris-HCl (pH 7.5), 70 mM $MgCl_2$, 1 mM DTT), 0.5 μl of 500 mM KCl, 0.5 μl of dNTP mixture (50 μM each), and 4.5 μl of Milli-Q water. After addition of 0.5 μl of Klenow fragment, the mixture was incubated at 37 °C for 10 min. The reaction was terminated by adding 1.5 μl of stop solution (160 mM EDTA, 0.7% SDS, 6 mg/ml proteinase K), and the samples were incubated at 37 °C for 30 min. Subsequently, 5.5 μl of the gel loading solution (30 mM EDTA, 0.05% bromophenol blue, 0.05% xylene cyanol, 97% formamide) was added to the samples. For pol δ, a ×10 reaction buffer containing 200 mM PIPES (pH 6.8), 20 mM $MgCl_2$, 10 mM 2-mercaptethanol, 200 μg/ml bovine serum albumin, and 50% glycerol was used instead of the buffer described above, and the reaction was carried out at 37 °C for 10 min. For other DNA polymerases, pol α, pol I, r*Taq*, and *Tth*, the constituent of each ×10 reaction buffer was altered as recommended by the suppliers.

The reaction using pol κ was performed as described above with some modifications. Briefly, an aliquot of 0.5 μl of this primer-annealed template (final 50 nM) was mixed with 0.5 μl of 10 × TLS buffer (250 mM Tris-HCl (pH 7.0), 50 mM $MgCl_2$, 50 mM DTT, 1 mg/ml bovine serum albumin), 0.5 μl of dNTP solution, and 3.0 μl of Milli-Q water. After addition of 0.5 μl of pol κ, the mixture was incubated at 30 °C for 20 min. The reac-